https://doi.org/10.1093/plcell/koad276 THE PLANT CELL 2024: 36: 367–382

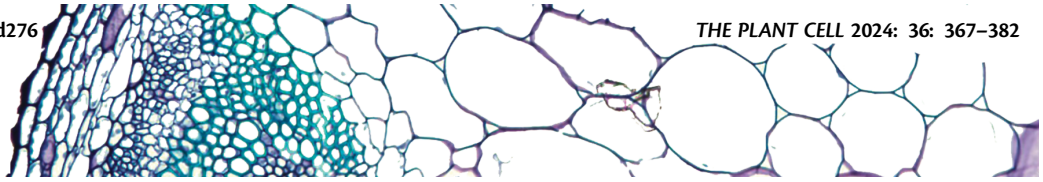

Research Article

S-nitrosylation of the transcription factor MYB30 facilitates nitric oxide–promoted seed germination in Arabidopsis

Hongyun Zhao [1], Liang Ma [3], Jialu Shen [1], Huapeng Zhou [2,*] and Yuan Zheng [1,*]

1 State Key Laboratory of Crop Stress Adaptation and Improvement, Key Laboratory of Plant Stress Biology, School of Life Sciences, Henan University, Kaifeng 475001, China
2 Key Laboratory of Bio-Resource and Eco-Environment of Ministry of Education, College of Life Sciences, Sichuan University, Chengdu 610064, China
3 State Key Laboratory of Plant Environmental Resilience, College of Biological Sciences, China Agricultural University, Beijing 100193, China

*Author for correspondence: zhengyuan051@163.com (Y.Z.), zhouhuapeng@scu.edu.cn (Hu.Z.)
The author responsible for distribution of materials integral to the findings presented in this article in accordance with the policy described in the Instructions for Authors (https://academic.oup.com/plcell/pages/General-Instructions) is Yuan Zheng.

Abstract

The gaseous signaling molecule nitric oxide (NO) plays an important role in breaking seed dormancy. NO induces a decrease in abscisic acid (ABA) content by transcriptionally activating its catabolic enzyme, the ABA 8′-hydroxylase *CYP707A2*. However, the underlying mechanism of this process remains unclear. Here, we report that the transcription factor MYB30 plays a critical role in NO-induced seed germination in Arabidopsis (*Arabidopsis thaliana*). *MYB30* loss-of-function attenuates NO-mediated seed dormancy breaking. MYB30 triggers a NO-induced decrease in ABA content during germination by directly promoting *CYP707A2* expression. NO induces *S*-nitrosylation at Cys-49 of MYB30 and enhances its transcriptional activity. Conversely, the ABA receptors PYRABACTIN RESISTANCE1 (PYR1)/PYR1-LIKE (PYL)/REGULATORY COMPONENTS OF ABA RECEPTORS (RCAR) interact with MYB30 and repress its transcriptional activity. ABA promotes the interaction between PYL4 and MYB30, whereas *S*-nitrosylation releases the PYL4-mediated inhibition of MYB30 by interfering with the PYL4-MYB30 interaction. Genetic analysis showed that *MYB30* functions downstream of *PYLs* during seed dormancy and germination in response to NO. Furthermore, *MYB30* mutation significantly represses the reduced dormancy phenotype and the enhanced *CYP707A2* expression of the *pyr1 pyl1 pyl2 pyl4* quadruple mutant. Our findings reveal that *S*-nitrosylation of MYB30 precisely regulates the balance of seed dormancy and germination, providing insights into the underlying mechanism of NO-promoted seed germination.

Introduction

Seed dormancy and germination are precisely controlled by exogenous and endogenous signals to prevent seed development under unfavorable conditions (Bentsink and Koornneef 2008; Graeber et al. 2012). The phytohormone abscisic acid (ABA) plays an essential role in the induction and maintenance of seed dormancy. Components related to ABA metabolism and signaling are extensively involved in the regulation of seed dormancy (Shu et al. 2016; Chen et al. 2020a; Sano and Marion-Poll 2021). For example, ABA biosynthesis mutants such as *9-CIS-EPOXYCAROTENOID DIOXYGENASE6* (*nced6*), *ABA DEFICIENT2* (*aba2*), and *ABSCISIC ALDEHYDE OXIDASE3* (*aao3*) contain less ABA and exhibit reduced dormancy (Seo et al. 2006), whereas ABA catabolism mutants, such as the ABA 8′-hydroxylase *cyp707a1* and *cyp707a2*, accumulate more ABA and subsequently show enhanced dormancy (Okamoto et al. 2006; Matakiadis et al. 2009). In addition, the ABA signaling positive regulator ABA-INSENSITIVE4 (ABI4)

Received August 28, 2023. Accepted October 04, 2023. Advance access publication November 1, 2023

enhances seed dormancy by directly repressing the expression of *CYP707A1* and *CYP707A2* (Söderman et al. 2000; Shu et al. 2013).

The gaseous signaling molecule nitric oxide (NO) also plays an important role in regulating seed dormancy and germination (Bethke et al. 2004, 2006). In plants, NO is produced by the nitrite-dependent NITRATE REDUCTASE1 and 2 (NIA1 and NIA2) and a pathway dependent on the NO-ASSOCIATED1 (NOA1) protein. The *nia1 nia2 noa1* triple mutant, which is deficient in NO generation, shows enhanced dormancy and delayed germination in response to exogenous ABA (Liu et al. 2009; Lozano-Juste and León 2010). Application of the exogenous NO donor sodium nitroprusside (SNP) breaks seed dormancy and promotes seed germination. In contrast, the NO scavenger 2-(4-carboxyphenyl)-4,4,5,5-tetramethylimidazoline-1-oxyl-3-oxide (cPTIO) arrests seed germination (Liu et al. 2009; Arc et al. 2013). The regulatory role of NO in seed dormancy depends on its antagonistic effect on ABA signaling. NO is released rapidly in the early hours of imbibition, and this rapid accumulation is required for the decrease in ABA. The NO-induced ABA decrease correlates with the regulation of the transcription of catabolic enzyme *CYP707A2*. The application of SNP dramatically induces the expression of *CYP707A2*, which subsequently leads to the catabolism of ABA as well as release from dormancy (Liu et al. 2009). However, the mediator of NO-induced *CYP707A2* expression and the mechanism by which NO regulates this process remain unclear.

NO exerts its physiological effects mainly through *S*-nitrosylation, which involves the covalent addition of an NO group to a thiol of cysteine (Cys) residue to form *S*-nitrosothiol (SNO). *S*-nitrosylation modulates protein activities by diverse mechanisms, including altering their subcellular localization, stability, enzymatic activity, and protein–protein interactions (Astier et al. 2011; Feng et al. 2019). NO antagonizes ABA-mediated inhibition of seed germination and seedling growth by the *S*-nitrosylation of the bZIP transcription factor ABSCISIC ACID INSENSITIVE5 (ABI5) (Albertos et al. 2015). ABI5 is considered as the final common repressor of seed germination in response to ABA and gibberellic acid (GA) (Lopez-Molina et al. 2002; Piskurewicz et al. 2008). The protein level and stability of ABI5 are enhanced by ABA. However, ABI5 protein decreases rapidly during seed germination, and this process is mediated by multiple ubiquitin E3 ligases, such as CULLIN4-based E3 ligases and RING-type E3 ligases KEEP ON GOING (KEG) and MYB30-INTERACTING E3 LIGASE1 (MIEL1) (Lee et al. 2010; Liu and Stone 2010; Seo et al. 2014; Nie et al. 2022). NO-induced *S*-nitrosylation of ABI5 at Cys-153 facilitates its degradation via the CULLIN4-based and KEG E3 ligases, thus promoting seed germination (Albertos et al. 2015).

The MYB transcription factor MYB30 was reported to act as a positive regulator of the hypersensitive response (HR) by activating the synthesis of very-long-chain fatty acids (VLCFAs) (Vailleau et al. 2002; Raffaele et al. 2008). Importantly, MYB30 was also identified as a negative regulator of ABA signaling in plants. Mutation of *MYB30* leads to hypersensitivity to ABA during seed germination and post-germination growth, whereas *MYB30*-overexpressing seeds are hyposensitive to ABA (Zheng et al. 2012). MYB30 can either directly repress the expression of ABA-responsive genes by binding to their promoters or interact with ABI5 to repress its transcriptional activity (Nie et al. 2022). The RING-type ubiquitin E3 ligases RING-H2 FINGER PROTEIN 2B (RHA2b) and MIEL1 participate in ABA signaling during seed germination through the regulation of MYB30 stability (Zheng et al. 2018; Nie et al. 2022). However, the function of MYB30 in seed dormancy and germination is still largely unknown.

In this study, we demonstrate that MYB30 participates in NO-induced seed dormancy breaking. MYB30 promotes *CYP707A2* expression by directly binding to its promoter, leading to ABA content decrease. NO-induced *S*-nitrosylation of MYB30 at Cys-49 enhances its transcriptional activation of *CYP707A2*. Conversely, ABA represses the transcriptional activity of MYB30 through the PYRABACTIN RESISTANCE1 (PYR1)/PYR1-LIKE (PYL)/REGULATORY COMPONENTS OF ABA RECEPTORS (RCAR) receptors (hereafter PYLs), whereas *S*-nitrosylation attenuates such repression by interfering with the PYL4-MYB30 interaction. These findings indicate that NO antagonistically regulates ABA by the *S*-nitrosylation of MYB30 and thus accurately regulates seed dormancy and germination.

Results

MYB30 positively regulates NO-mediated seed dormancy breaking

To investigate the role of MYB30 in seed dormancy, a germination assay was conducted with freshly harvested seeds of *MYB30*-knockout mutant plants *myb30-1* and *myb30-2* (Supplemental Fig. S1; Zheng et al. 2012). The *myb30* mutant seeds exhibited lower germination rates than that of the wild-type (WT) seeds (Fig. 1, A and B), suggesting that MYB30 participates in seed dormancy regulation. The application of the NO donor *S*-nitrosoglutathione (GSNO) increased the germination rates of both WT and *myb30* mutants, but the germination rates of *myb30* mutant seeds were still lower than those of WT seeds (Fig. 1, A and B). In contrast, the germination rates decreased in the presence of the NO scavenger cPTIO. However, WT seeds still showed higher germination rates than those of *myb30* mutants (Fig. 1, A and B). Compared with the WT, the change in germination rates of *myb30* mutants in response to GSNO or cPTIO was much lower (Fig. 1C), suggesting that MYB30 is involved in the response to NO during seed dormancy and germination. Moreover, the *MYB30*-overexpressing seeds *Pro35S:MYC-MYB30* (*MYC-MYB30*) exhibited a less dormant phenotype, and the germination rates of *MYC-MYB30* under both GSNO and cPTIO treatments were all higher than those of the WT (Supplemental Figs. S1 and S2). These results suggest that MYB30 regulates seed dormancy and is involved in NO-mediated seed dormancy breaking.

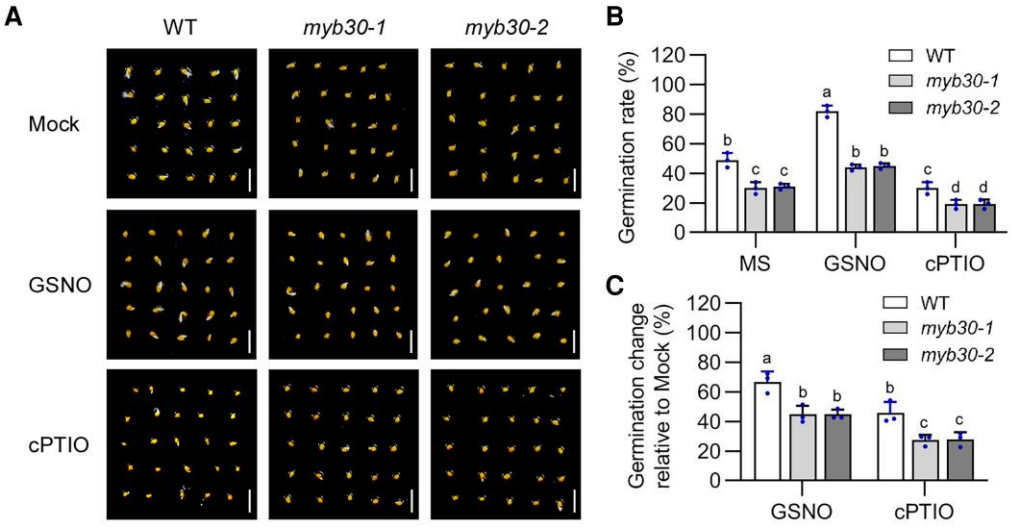

Figure 1. MYB30 positively regulates NO-mediated seed dormancy breaking. **A)** Dormancy phenotypes of freshly harvested seeds of the WT and *myb30* mutants grown on 0.3% agar without (Mock) or with 100 μM GSNO/cPTIO for 2 d. WT: wild type. Scale bars = 2 mm. **B)** Germination rates of the seeds shown in **A)**. **C)** Germination rate changes under GSNO and cPTIO treatments relative to Mock. The value was obtained by comparing the difference between the treated and mock germination rates with the germination rate of the mock. For **B)** and **C)**, data represent the mean of 50 seeds from at least 3 independent experiments ± SD. Different letters above the columns indicate significant differences based on ANOVA ($P < 0.05$).

MYB30 promotes seed dormancy breaking by directly activating *CYP707A2* expression for ABA catabolism

Previous studies have shown that NO promotes the catabolism of ABA during germination by inducing the expression of the ABA catabolic gene *CYP707A2* (Liu et al. 2009). We therefore quantified the transcript levels of genes encoding ABA biosynthesis (*ABA1*, *AAO3*, *NCED3*, and *NCED9*) and catabolic (*CYP707A1*, *CYP707A2*, and *CYP707A3*) enzymes in the WT and *myb30-2* mutant using RT-qPCR. The expression levels of ABA biosynthesis genes were similar in the WT and *myb30-2* mutant seeds (Supplemental Fig. S3A). However, the increase in *CYP707A2* and *CYP707A3* expression during imbibition was substantially repressed in the *myb30-2* mutant (Fig. 2A; Supplemental Fig. S3B). Consistent with these results, the content of endogenous ABA in germinating seeds was higher in the *myb30-2* mutant than in the WT (Fig. 2B), suggesting that MYB30 participates in NO-induced ABA catabolism.

We identified a MYB30-binding site (AACAAAC; Li et al. 2009; Liao et al. 2017) in the promoter of *CYP707A2* (Supplemental Fig. S4A), suggesting that *CYP707A2* may be a target of MYB30. In the electrophoretic mobility shift assay (EMSA), the GST-tagged N-terminal region (residues 1 to 149, containing R2R3-MYB DNA-binding domain) of MYB30 (MYB30N) bound to the *CYP707A2* promoter fragment containing the MYB30-binding site. This binding was blocked by an unlabeled probe but not by a probe with mutations in the MYB30-binding site (Fig. 2C; Supplemental Fig. S4B), indicating the specific binding of MYB30 to the *CYP707A2* promoter.

To confirm the association of MYB30 with the *CYP707A2* promoter in planta, transient expression assays and chromatin immunoprecipitation (ChIP)-qPCR were conducted. The promoter of *CYP707A2* was fused to the *luciferase* (*LUC*) gene as the reporter and *REN* (*Renilla LUC*) gene driven by *35S* promoter as the internal control. The GFP and MYB30-GFP under the control of the *35S* promoter were used as effectors. Compared with GFP, MYB30-GFP significantly activated the expression of *ProCYP707A2:LUC* (Fig. 2D; Supplemental Fig. S4C). For ChIP-qPCR, WT and *Pro35S:MYC-MYB30* transgenic plants were used for analysis. The fragment containing the MYB30-binding site was strongly enriched by the anti-MYC antibody (Fig. 2E). Taken together, these data demonstrate that MYB30 activates the expression of *CYP707A2* by directly binding to its promoter.

To evaluate the importance of *CYP707A2* expression in MYB30-mediated seed dormancy regulation, we overexpressed *CYP707A2* in the *myb30-2* mutant and assessed the dormancy phenotype of *Pro35S:CYP707A2-GFP/myb30-2* (Supplemental Fig. S4D). Our results showed that overexpression of *CYP707A2* significantly increased the germination rates of fresh seeds of the *myb30-2* mutant. Moreover, compared with the WT, these seeds showed less dormancy (Fig. 2, F and G). These results suggest that the regulation of *CYP707A2* expression by MYB30 is crucial for its function in seed dormancy.

NO-activated *CYP707A2* expression and ABA catabolism are partially dependent on MYB30

Next, the role of MYB30 in NO-mediated activation of *CYP707A2* expression was investigated. In the *myb30-2* mutant, activation of *CYP707A2* by GSNO was inhibited, whereas the repression by cPTIO was more pronounced (Fig. 2H). Compared with the WT, the ABA content in the *myb30-2* mutant was also higher under the treatments of GSNO and cPTIO (Fig. 2B), suggesting that MYB30 participates in NO-induced ABA catabolism. Consistent with the finding

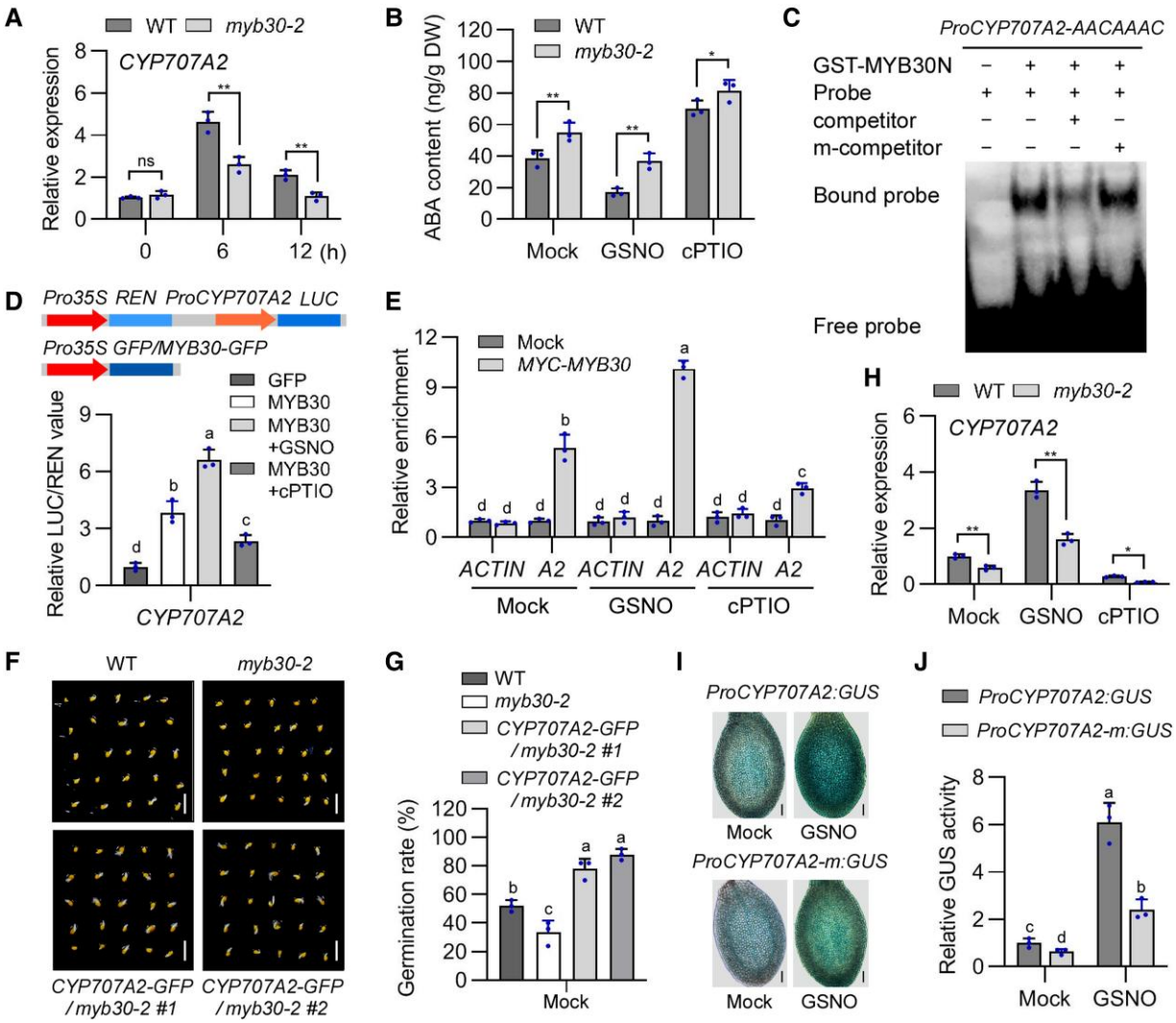

Figure 2. MYB30 promotes NO-mediated seed dormancy breaking by directly activating the expression of *CYP707A2* for ABA catabolism. **A)** Expression of *CYP707A2* during germination was identified by RT-qPCR. Freshly harvested seeds of the WT and *myb30-2* mutant imbibed in water for the indicated time were used for RNA extraction. **B)** ABA content in imbibed seeds of the WT and *myb30-2* mutant. Freshly harvested seeds imbibed in water without or with 100 μM GSNO/cPTIO for 6 h were used for analysis. DW: dry weight. **C)** EMSAs showing that GST-MYB30N directly binds to the AACAAAC motif in the *CYP707A2* promoter in vitro. **D)** The effects of MYB30 on *CYP707A2* expression were examined by transiently expressing GFP (control) or MYB30-GFP with *ProCYP707A2:LUC* in Arabidopsis protoplasts. +GSNO/+cPTIO represents treatment with 100 μM GSNO/cPTIO for 3 h. The relative LUC/REN ratios were analyzed. **E)** ChIP-qPCR analysis of the enrichment of MYB30 at *CYP707A2* loci. WT and *Pro35S:MYC-MYB30* seeds imbibed in water (Mock) or water containing 100 μM GSNO/cPTIO for 12 h were used for analysis. The *ACTIN2* (*ACTIN*) was used as a reference gene. **F)** Dormancy phenotypes of freshly harvested seeds of the WT, *myb30-2*, and *Pro35S:CYP707A2-GFP/myb30-2* (*CYP707A2-GFP/myb30-2*). Scale bars = 2 mm. **G)** Germination rates of the seeds shown in **F)**. **H)** Expression of *CYP707A2* under GSNO and cPTIO treatment. Freshly harvested seeds imbibed in water (Mock) or water containing 100 μM GSNO/cPTIO for 6 h were used for RNA extraction. **I)** GUS staining images of *ProCYP707A2:GUS* and *ProCYP707A2-m:GUS* transgenic reporter seeds. Scale bars = 100 μm. **J)** Relative GUS activity of the seeds in **I)**. For **A)**, **B)**, and **H)**, data represent means ± SD ($n = 3$); statistical significance of the measurements was analyzed by Student's *t* test (**$P < 0.01$, *$P < 0.05$). For **D)**, **E)**, **G)**, and **J)**, data represent means ± SD ($n = 3$); different letters above the columns indicate significant differences based on ANOVA ($P < 0.05$).

that NO promotes the expression of *CYP707A2*, GSNO treatment enhanced the MYB30-mediated activation of *CYP707A2*, whereas this activation was significantly repressed after the application of cPTIO (Fig. 2D; Supplemental Fig. S4C). Moreover, the enrichment of the *CYP707A2* promoter by MYB30 was significantly enhanced by the application of GSNO but reduced by cPTIO treatment (Fig. 2E), suggesting that MYB30 participates in the regulation of *CYP707A2* expression in response to NO.

We further confirmed whether the expression and stability of MYB30 were also regulated by NO. The expression of *MYB30* in response to NO was assessed using the seeds

imbibed in water (Mock) or water containing 100 μM GSNO. RT-qPCR analysis showed that there was no significant difference of *MYB30* expression between Mock and GSNO treatment (Supplemental Fig. S5A), suggesting that the expression of *MYB30* does not respond to NO. The stability of MYB30 in response to NO was evaluated using 7-d-old *Pro35S:MYC-MYB30* seedlings treated with GSNO alone or together with cycloheximide (CHX), a protein synthesis inhibitor (Chen et al. 2022). Our immunoblot data showed that the application of GSNO did not affect the protein level of MYB30 (Supplemental Fig. S5, B and C). These results suggest that NO regulates the transcriptional activity rather than the expression and stability of MYB30.

To clarify whether the MYB30-binding site in the *CYP707A2* promoter is critical for the response to NO in seeds, stable transgenic β-glucuronidase (GUS) reporter lines, *ProCYP707A2:GUS* and *ProCYP707A2-m:GUS*, in which *GUS* expression was under the control of the *CYP707A2* native promoter or mutated promoter (with AACAAAC mutated to ATGTTAC) were constructed. In agreement with *CYP707A2* expression induced by the application of GSNO, GSNO treatment also increased the GUS staining and GUS activity of *ProCYP707A2:GUS* seeds (Fig. 2, I and J). Compared with *ProCYP707A2:GUS* seeds, both GUS staining and activity in *ProCYP707A2-m:GUS* seeds were dramatically reduced after germination or under GSNO treatment (Fig. 2, I and J), suggesting that the MYB30-binding site plays an important role in *CYP707A2* expression during germination and in response to NO. Taken together, our data demonstrate that NO regulates *CYP707A2* expression by modulating the transcriptional activity of MYB30.

S-nitrosylation of MYB30 is critical for its transcriptional activity during NO-induced seed germination

As *S*-nitrosylation is an important way for the NO signal to exert its function, we explored whether MYB30 can be *S*-nitrosylated. The biotin-switch assay revealed that GSNO induced *S*-nitrosylation of the recombinant His-MYB30N protein (Fig. 3A). *S*-nitrosylation of MYB30 was also detected in planta, and the level of *S*-nitrosylated MYB30 was increased in the *gsnor1-3* (*GSNO REDUCTASE1*) mutant, which contained a higher endogenous NO content (Fig. 3B). Furthermore, during germination, the *S*-nitrosylation level of MYB30 increased, which was promoted by GSNO and inhibited by cPTIO (Fig. 3C). These results demonstrate that *S*-nitrosylation of MYB30 occurs in planta and is precisely controlled during germination.

A mass spectrometric analysis of MYB30N recombinant protein identified Cys-6, Cys-7, and Cys-49 as *S*-nitrosylated residues (Supplemental Fig. S6). As Cys-49 is located in the MYB DNA-binding domain of MYB30 (Supplemental Fig. S6A), we chose Cys-49 residue for further analysis. Our analysis showed that substitution of Cys-49 with serine (Ser; MYB30^{C49S}) substantially reduced the *S*-nitrosylation level of His-MYB30N (Fig. 3D), and the *S*-nitrosylation level of MYC-MYB30^{C49S} was substantially lower than that of MYC-MYB30 (Fig. 3E; Supplemental Fig. S7, A and B). In addition, compared with that of MYC-MYB30, the *S*-nitrosylation level of MYC-MYB30^{C49S} was lower during germination (Fig. 3F). Therefore, we further explored the function of the MYB30 Cys-49 residue.

Tryptophan (W) has been shown to mimic an *S*-nitrosylated Cys (Palmer et al. 2008; Feng et al. 2013). Thus, the Cys-49 to Try-49 substitution was used to analyze the effect of *S*-nitrosylation on MYB30 (Supplemental Fig. S7, A and B). We first evaluated the transcriptional activity of MYB^{C49W} using a transient expression assay. *ProCYP707A2:LUC* was transiently expressed in WT, *Pro35S:MYC-MYB30*, and *Pro35S:MYC-MYB30*^{C49W} protoplasts. The expression of *LUC* was substantially higher in *Pro35S:MYC-MYB30*^{C49W} protoplasts than in *Pro35S:MYC-MYB30* (Fig. 3G). We also evaluated the transcriptional activity of MYB30 and MYB30^{C49W} using ChIP-qPCR and found that the enrichment of MYB30^{C49W} on the *CYP707A2* promoter was greater than that of MYB30 (Fig. 3H), suggesting that *S*-nitrosylation at the Cys-49 residue enhances the transcriptional activity of MYB30.

To determine the importance of MYB30 Cys-49 *S*-nitrosylation, the function of MYB30^{C49W} in seed dormancy was investigated. MYB30 and MYB30^{C49W} were expressed in the *myb30-2* mutant under the control of the native *MYB30* promoter (Supplemental Fig. S7C). The data showed that the enhanced dormancy of the *myb30-2* mutant was fully rescued by the expression of *MYB30* (*MYB30*). Moreover, the *ProMYB30:MYB30* seeds exhibited phenotypes similar to those of the WT in response to GSNO and cPTIO. However, the expression of *MYB30*^{C49W} (*C49W*) resulted in a reduction in seed dormancy compared with that of the WT under all conditions (Fig. 3I). Taken together, our results indicate that *S*-nitrosylation of MYB30 at Cys-49 enhances its transcriptional activity, thus promoting seed germination.

PYLs interact with MYB30 and repress its transcriptional activity

As MYB30 directly activates *CYP707A2* expression, we hypothesized that the function of MYB30 should be repressed during seed dormancy, as there is a high level of endogenous ABA in seeds. We revealed the interaction between MYB30 and the core components of ABA signaling, such as PYL ABA receptors (Ma et al. 2009; Park et al. 2009), through a bimolecular fluorescence complementation (BiFC) assay. Encouragingly, we found that PYLs can directly interact with MYB30. Specifically, PYL3, PYL4, PYL8, PYL10, PYL11, and PYL12 interacted with MYB30 in the nucleus in our assay (Fig. 4A; Supplemental Fig. S8A). Because of its important role in regulating ABA signaling during germination (Park et al. 2009; Wang et al. 2020), PYL4 was selected to further explore the relationships between PYLs and MYB30.

MYC-MYB30 and PYL4-GFP were transiently coexpressed in *Nicotiana benthamiana* leaves, and coimmunoprecipitation (Co-IP) assays were performed. MYC-MYB30 was precipitated only when it was coexpressed with PYL4-GFP

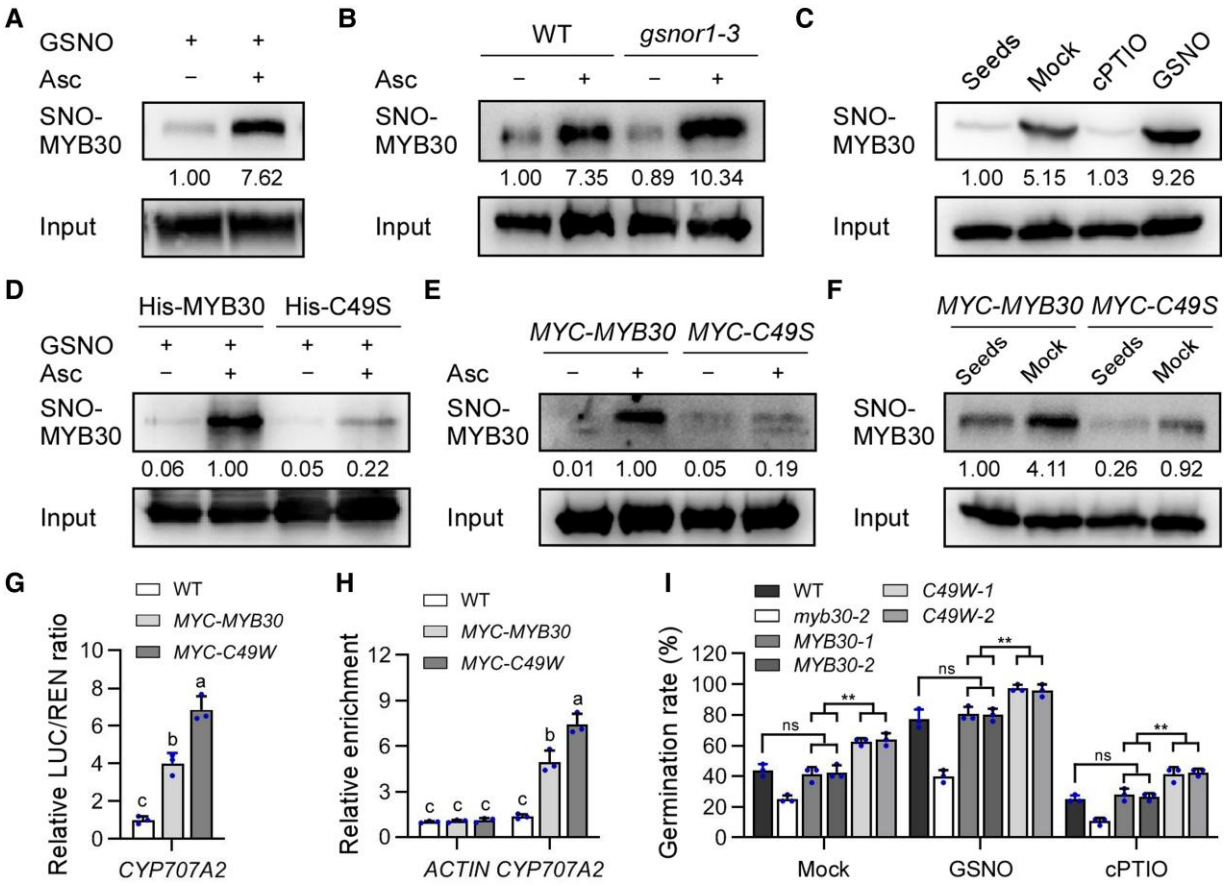

Figure 3. *S*-nitrosylation of MYB30 is critical for its transcriptional activity during NO-induced seed germination. **A)** Analysis of *S*-nitrosylation of His-MYB30N (SNO-MYB30) treated with GSNO by an in vitro *S*-nitrosylation assay. A sample without sodium ascorbate (Asc) treatment is shown as a negative control. **B)** Analysis of MYB30 *S*-nitrosylation in *Pro35S:MYC-MYB30*/WT and *Pro35S:MYC-MYB30*/*gsnor1-3* seeds by an in vivo *S*-nitrosylation assay. Samples without Asc treatment served as negative controls. **C)** Analysis of MYB30 *S*-nitrosylation in dormant seeds and seeds imbibed in water (Mock) or water containing 100 μM GSNO/cPTIO for 12 h. **D)** Analysis of His-MYB30 and MYB30^{C49S} *S*-nitrosylation by an in vitro *S*-nitrosylation assay. **E)** Analysis of MYB30 and MYB30^{C49S} *S*-nitrosylation using *Pro35S:MYC-MYB30* (*MYC-MYB30*) and *Pro35S:MYC-MYB30*^{C49S} (*MYC-C49S*) seeds by an in vivo *S*-nitrosylation assay. **F)** Analysis of MYB30 and MYB30^{C49S} *S*-nitrosylation in dormant seeds and seeds imbibed in water for 12 h. For **A)** to **F)**, quantification of the *S*-nitrosylation level is shown below the blot. The relative band intensities of *S*-nitrosylation were normalized to the loading control. The ratio of the first band (**A**–**C** and **F**) or second band (**D** and **E**) was set to 1. **G)** The activation of *CYP707A2* expression by MYB30 and MYB30^{C49W} was analyzed by a transient expression assay. *ProCYP707A2:LUC* was transiently expressed in protoplasts of WT, *Pro35S:MYC-MYB30*, and *Pro35S:MYC-MYB30*^{C49W} (*MYC-C49W*) leaves. The relative LUC/REN ratios were analyzed. **H)** ChIP-qPCR analysis of the enrichment of MYB30 and MYB30^{C49W} at *CYP707A2* loci. For **G)** and **H)**, different letters above the columns indicate significant differences based on ANOVA ($P < 0.05$). Error bars in **G)** and **H)** represent SD from 3 independent assays. **I)** Germination rates of freshly harvested seeds of WT, *myb30-2* mutant, *ProMYB30:MYB30*/*myb30-2* (*MYB30*), and *ProMYB30:MYB30*^{C49W}/*myb30-2* (*C49W*) grown on 0.3% agar (Mock) with or without 100 μM GSNO/cPTIO. Data represent means ± SD ($n = 3$). The statistical significance of the measurements was analyzed by ANOVA (**$P < 0.01$).

(Supplemental Fig. S8B). To more accurately evaluate the relationship between PYL4 and MYB30 during germination, the PYL4-MYB30 interaction was also tested in seeds via Co-IP. To this end, *Pro35S:PYL4-GFP Pro35S:MYC-MYB30* transgenic plants were generated by crossing *Pro35S:MYC-MYB30* with *Pro35S:PYL4-GFP* (Supplemental Fig. S7D). Seeds of *Pro35S:MYC-MYB30*, *Pro35S:PYL4-GFP*, and *Pro35S:MYC-MYB30 Pro35S:PYL4-GFP* were used for protein extraction. Immunoblot analysis indicated that MYC-MYB30 coimmunoprecipitated with PYL4-GFP (Fig. 4B), suggesting that PYL4 interacts with MYB30 in seeds. Furthermore, we also assessed the effect of ABA on the PYL4-MYB30 interaction through a LUC complementation imaging (LCI) assay. PYL4 and MYB30 were fused to the N-terminal half (nLUC) and the C-terminal half (cLUC) of LUC, respectively. LUC activity was detected only when PYL4 was co-transformed with MYB30 and ABA treatment enhanced the LUC intensity (Fig. 4C; Supplemental Fig. S8C). Moreover, the amount of MYB30 protein that precipitated with PYL4 also increased after ABA treatment (Fig. 4D), suggesting that the interaction between PYL4 and MYB30 responds to ABA.

As PYL4 and MYB30 perform opposite functions in ABA signaling, we investigated whether PYL4 interferes with the

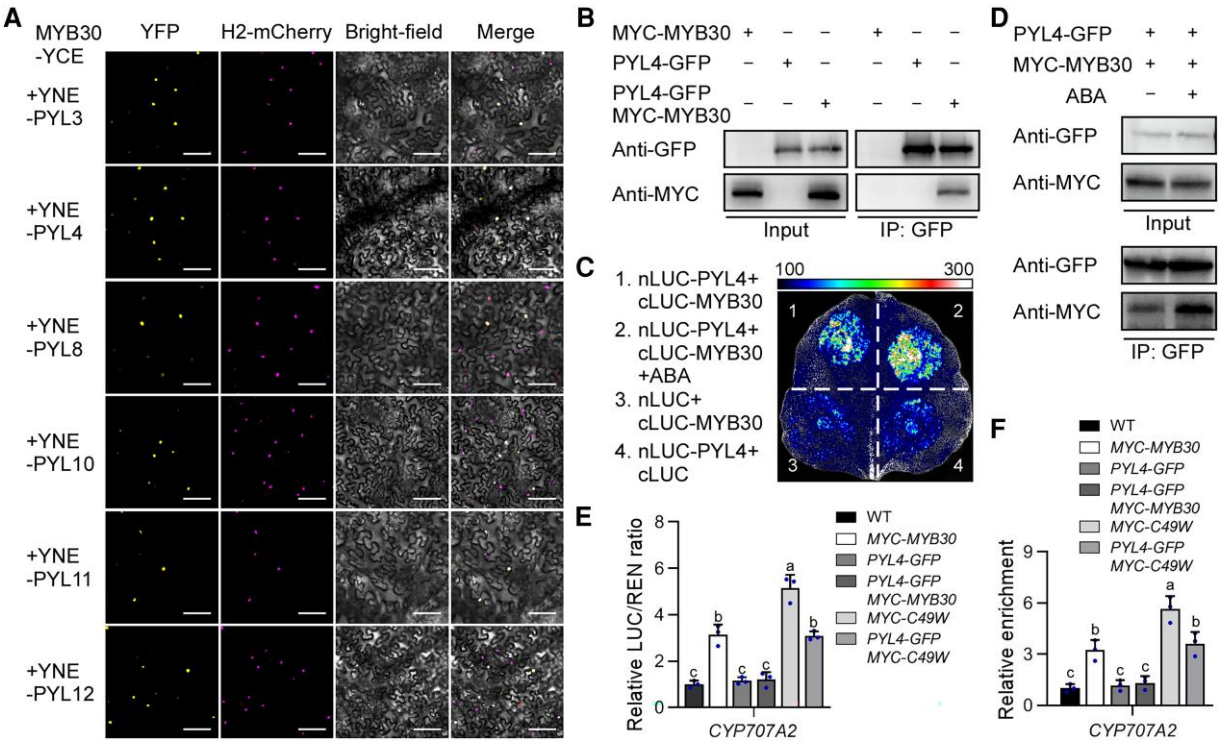

Figure 4. PYLs interact with MYB30 and repress its transcriptional activity. **A)** BiFC assay to evaluate the interaction between PYLs and MYB30. YNE-PYLs and MYB30-YCE were transiently coexpressed in *N. benthamiana* leaves. Scale bars = 100 μm. **B)** Co-IP assay to evaluate the PYL4-MYB30 interaction in seeds. Proteins were extracted from the indicated transgenic seeds and purified with anti-GFP agarose beads. **C)** LCI assay to evaluate the PYL4-MYB30 interaction. The *nLUC-PYL4* and *cLUC-MYB30* constructs were transiently expressed in *N. benthamiana* leaves for 2 d and then treated without or with 10 μM ABA for 3 h. **D)** Co-IP assay to evaluate the PYL4-MYB30 interaction under ABA treatment. PYL4-GFP and MYC-MYB30 were transiently expressed in *N. benthamiana* leaves. For the ABA treatment, leaves were treated with 10 μM ABA for 3 h before protein extraction. **E)** The effect of PYL4 on the activation of *CYP707A2* expression by MYB30 and MYB30^{C49W} was analyzed by a transient expression assay. *ProCYP707A2:LUC* was transiently expressed in protoplasts of WT and multiple transgenic plants. The relative LUC/REN ratios were analyzed. **F)** The effect of PYL4 on the enrichment of MYB30 and MYB30^{C49W} on the *CYP707A2* promoter was analyzed by ChIP-qPCR using WT and multiple transgenic plants. For **E)** and **F)**, data represent means ± SD ($n = 3$); different letters above the columns indicate significant differences based on ANOVA ($P < 0.05$).

transcriptional activity of MYB30. *ProCYP707A2:LUC* was transiently expressed in protoplasts of multiple genotypes to test the transcriptional activity of MYB30. *LUC* expression in *Pro35S:PYL4-GFP Pro35S:MYC-MYB30* was significantly lower than that in *Pro35S:MYC-MYB30*, suggesting that the transcriptional activation of *CYP707A2* by MYB30 is attenuated by PYL4 (Fig. 4E). ChIP analysis was conducted to test whether PYL4 affects the binding of MYB30 to the *CYP707A2* promoter. Compared with *Pro35S:MYC-MYB30*, the enrichment of MYB30 on the *CYP707A2* promoter was reduced in *Pro35S:PYL4-GFP Pro35S:MYC-MYB30* (Fig. 4F). These observations suggest that PYL4 interferes with the binding of MYB30 to the promoter of *CYP707A2*.

MYB30 functions downstream of PYLs in seed dormancy, and *S*-nitrosylation of MYB30 attenuates PYL4-mediated inhibition of MYB30 function

To further confirm the connection between PYLs and MYB30, the genetic relationship between *PYLs* and *MYB30* during seed dormancy and germination was analyzed. The quadruple mutant *pyr1 pyl1 pyl2 pyl4* (*pyr1 pyl124*), which shows strong insensitivity to exogenous ABA during germination, was used for analysis (Park et al. 2009). The *pyr1 pyl124 myb30-2* quintuple mutant was acquired by crossing *pyr1 pyl124* with *myb30-2*. Our phenotypic analysis showed that the *pyr1 pyl124* mutant seeds exhibited less dormancy than the WT seeds, and the germination rates of *pyr1 pyl124* under both GSNO and cPTIO treatments were all higher than those of the WT (Fig. 5, A and B). Moreover, the expression of *CYP707A2* was also enhanced in the *pyr1 pyl124* mutant (Fig. 5C). Further analysis showed that the mutation of *MYB30* significantly repressed the reduced dormant phenotype and the enhanced *CYP707A2* expression of the *pyr1 pyl124* mutant (Fig. 5, A to C), suggesting that *MYB30* functions downstream of *PYLs* during seed dormancy and germination in response to NO.

We next examined whether *S*-nitrosylation activates MYB30 by attenuating the inhibition of MYB30 by PYL4. *Pro35S:MYC-MYB30*^{C49W} and *Pro35S:PYL4-GFP Pro35S:MYC-MYB30*^{C49W} transgenic plants were used for analysis

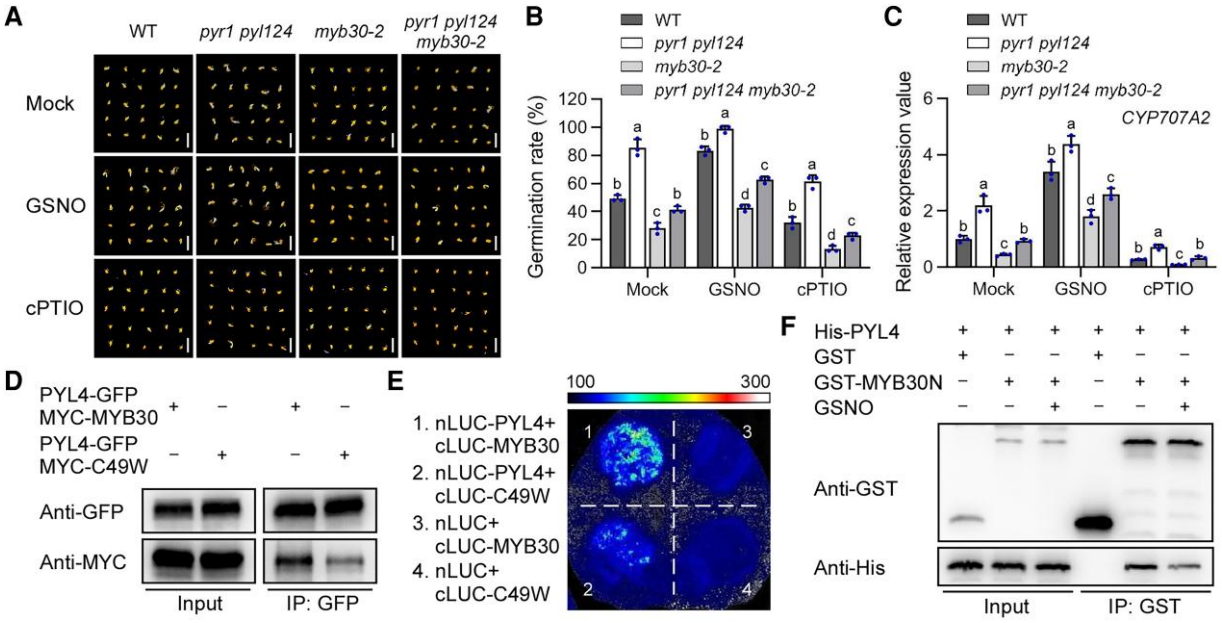

Figure 5. MYB30 functions downstream of PYLs in seed dormancy and *S*-nitrosylation of MYB30 attenuates PYL4-mediated inhibition of MYB30 function. **A)** Dormancy phenotypes of freshly harvested seeds of the WT, *myb30-2*, *pyr1 pyl124*, and *pyr1 pyl124 myb30-2* mutants grown on 0.3% agar without (Mock) or with 100 μM GSNO/cPTIO for 2 d. Scale bars = 2 mm. **B)** Germination rates of the seeds shown in **A)**. **C)** Expression of *CYP707A2* during germination under GSNO and cPTIO treatment. Freshly harvested seeds imbibed in water (Mock) or water containing 100 μM GSNO/cPTIO for 6 h were used for RNA extraction. For **B)** and **C)**, data represent means ± SD ($n = 3$); different letters above the columns indicate significant differences based on ANOVA ($P < 0.05$). **D)** The interactions between PYL4 and MYB30/MYB30^{C49W} were analyzed by a Co-IP assay using seeds of *Pro35S:PYL4-GFP Pro35S:MYC-MYB30* (*PYL4-GFP MYC-MYB30*) and *Pro35S:PYL4-GFP Pro35S:MYC-MYB30^{C49W}* (*PYL4-GFP MYC-C49W*) transgenic plants. **E)** The interactions between PYL4 and MYB30/MYB30^{C49W} were analyzed by LCI. **F)** In vitro pull-down assay for MYB30 and PYL4 interaction. His-tagged PYL4 was incubated with GST or GST-tagged MYB30N. Proteins were purified using anti-GST agarose and detected through immunoblot analysis using anti-GST and anti-His antibodies, respectively. For GSNO treatment, MYB30 protein was treated with 200 μM GSNO for 3 h before purified.

(Supplemental Fig. S7D). Our results showed that *ProCYP707A2:LUC* expression in *Pro35S:PYL4-GFP Pro35S:MYC-MYB30^{C49W}* protoplasts was less repressed than that in *Pro35S:PYL4-GFP Pro35S:MYC-MYB30* (Fig. 4E). In addition, the enrichment of MYB30^{C49W} on the *CYP707A2* promoter in *Pro35S:PYL4-GFP Pro35S:MYC-MYB30^{C49W}* was less affected than the block of MYB30 by PYL4 in *Pro35S:PYL4-GFP Pro35S:MYC-MYB30* (Fig. 4F). These results indicate that *S*-nitrosylation attenuates the repression of MYB30 by PYL4.

We hypothesized that *S*-nitrosylation may function by modulating the PYL4-MYB30 interaction. Seeds of *Pro35S:PYL4-GFP Pro35S:MYC-MYB30* and *Pro35S:PYL4-GFP Pro35S:MYC-MYB30^{C49W}* transgenic plants were used for a Co-IP assay. Immunoblot analysis indicated that the interaction between PYL4 and MYB30^{C49W} was substantially weaker than that between PYL4 and MYB30 in seeds (Fig. 5D). In addition, the LUC intensity resulting from the PYL4-MYB30^{C49W} interaction was significantly lower than that caused by the PYL4-MYB30 interaction (Fig. 5E; Supplemental Fig. S8D), suggesting that *S*-nitrosylation attenuates the interaction between PYL4 and MYB30. Next, an in vitro pull-down assay was performed to evaluate the PYL4-MYB30 interaction in response to NO (Chen et al. 2022). His-PYL4 and GST-MYB30N recombinant proteins purified from *Escherichia coli* were used. Our results validated that GST-MYB30N can interact with His-PYL4 and that the application of GSNO on MYB30 reduced the PYL4-MYB30 interaction (Fig. 5F). Taken together, these experiments demonstrate that *S*-nitrosylation enhances the transcriptional activity of MYB30 by interfering with the MYB30-PYL4 interaction.

S-nitrosylation of MYB30 attenuates PYL4-mediated inhibition of seed germination in response to ABA

To further test the effect of PYL4 on the transcriptional activity of MYB30, another MYB30 target, the ABA-responsive gene *EARLY METHIONINE-LABELED1* (*EM1*), was used for analysis (Nie et al. 2022). As shown in Fig. 6A, the *LUC* expression driven by the *EM1* promoter was repressed in *Pro35S:MYC-MYB30* and *Pro35S:MYC-MYB30^{C49W}* protoplasts but enhanced in *Pro35S:PYL4-GFP* protoplasts. However, the expression of *LUC* in *Pro35S:PYL4-GFP Pro35S:MYC-MYB30* was similar to that in *Pro35S:PYL4-GFP*, but *LUC* expression in *Pro35S:PYL4-GFP Pro35S:MYC-MYB30^{C49W}* was more similar to that in *Pro35S:MYC-MYB30^{C49W}*. In the ChIP assay, the enrichment of the *EM1* promoter by MYB30 significantly decreased in *Pro35S:PYL4-GFP Pro35S:MYC-MYB30* seeds, but the enrichment of MYB30^{C49W} was only slightly affected in *Pro35S:PYL4-GFP Pro35S:MYC-MYB30^{C49W}* (Fig. 6B). These results indicate that *S*-nitrosylation also attenuates the repression of MYB30 by PYL4 on ABA-responsive gene expression.

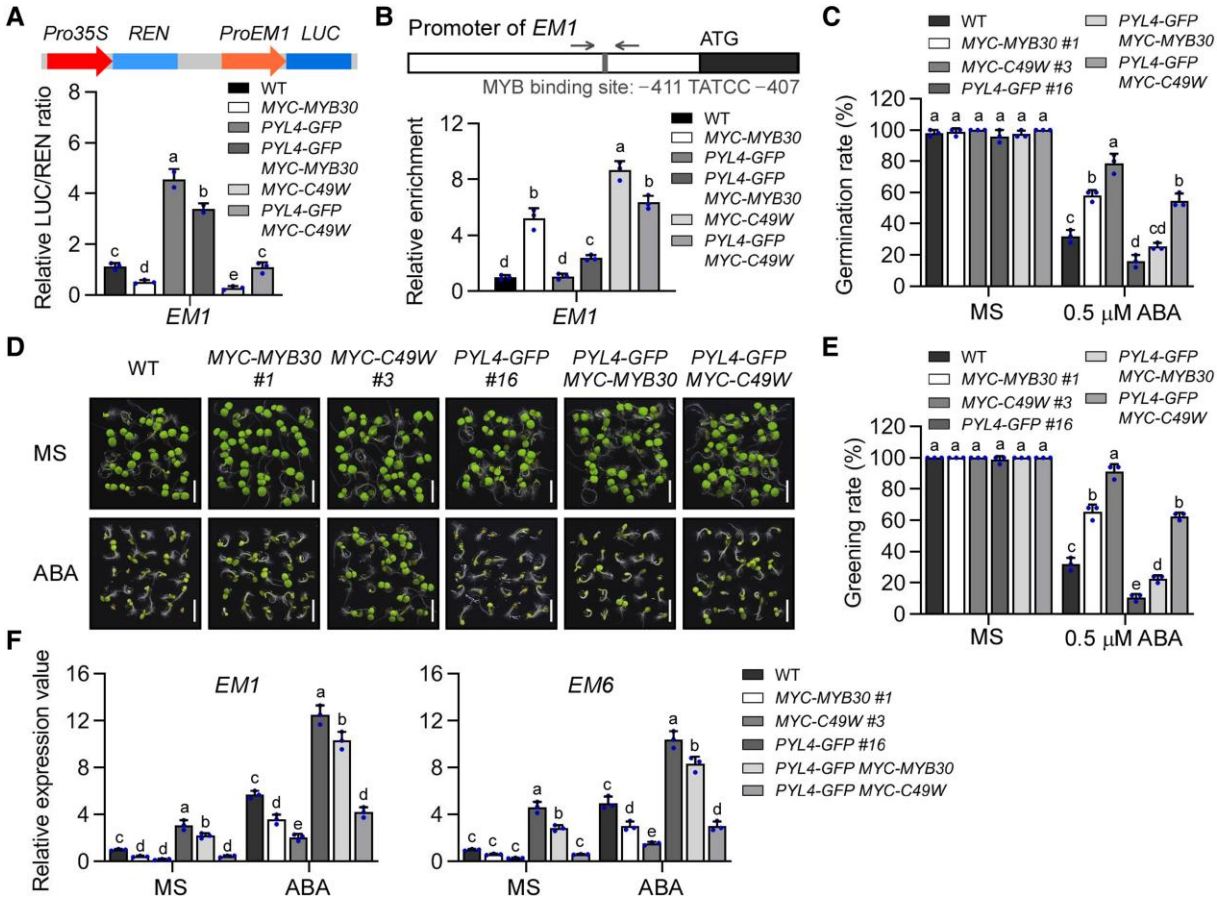

Figure 6. *S*-nitrosylation of MYB30 attenuates PYL4-mediated inhibition of seed germination in response to ABA. **A)** The effect of PYL4 on the repression of *EM1* expression by MYB30 and MYB30^{C49W} was analyzed by a transient expression assay. *ProEM1:LUC* was transiently expressed in protoplasts of WT and multiple transgenic plants. The relative LUC/REN ratios were analyzed. **B)** The effect of PYL4 on the enrichment of MYB30 and MYB30^{C49W} on the *EM1* promoter was analyzed by ChIP-qPCR using WT and multiple transgenic plants. The arrows depict the location of amplified fragment of ChIP-qPCR. The position of MYB-binding site is also indicated. **C)** Germination percentages of MYB30- and PYL4-related transgenic plants in response to ABA. Seed germination on MS medium without or with 0.5 μM ABA was recorded after 3 d of stratification. **D)** Seedlings of various genotypes grown on MS medium containing 0.5 μM ABA. Scale bars = 3 mm. **E)** Percentages of greening cotyledon of multiple genotypes. **F)** *EM1* and *EM6* expression levels in multiple genotypes were identified by RT-qPCR. Seeds grown on MS medium without (Mock) or with 10 μM ABA for 24 h were used for RNA extraction. Three independent biological replicates were averaged. For **A)** to **C)**, **E)**, and **F)**, different letters above the columns indicate significant differences based on ANOVA ($P < 0.05$). Error bars indicate the mean ± SD ($n = 3$).

In addition, it has been reported that MYB30 negatively regulates ABA signaling by interacting with ABI5 to repress its transcriptional activity. MYB30, MYB30^{C49W}, and ABI5 were coexpressed with *ProEM1:LUC* in Arabidopsis protoplasts to assess the effect of MYB30 *S*-nitrosylation on the transcriptional activity of ABI5. Our results showed that MYB30^{C49W} repression of ABI5-mediated *EM1* activation was significantly stronger than that of MYB30 (Supplemental Fig. S9A). Further analysis showed that the interaction between MYB30^{C49W} and ABI5 was enhanced compared with the MYB30-ABI5 interaction in the yeast 2-hybrid assay (Supplemental Fig. S9B), suggesting that *S*-nitrosylation may promote the inhibition of ABI5 by MYB30 by enhancing their interaction.

Finally, the function of MYB30 *S*-nitrosylation in ABA-mediated inhibition of seed germination was addressed. Overexpression of *MYB30* caused hyposensitivity to ABA at both the germination and postgermination stages, while overexpression of *MYB30*^{C49W} resulted in a more insensitive phenotype. In contrast, seeds overexpressing *PYL4* were more sensitive to ABA. When both *PYL4* and *MYB30* were overexpressed, the transgenic seeds exhibited an ABA-hypersensitive phenotype similar to that of *Pro35S:PYL4-GFP*. However, seeds overexpressing both *PYL4* and *MYB30*^{C49W} remained insensitive to ABA (Fig. 6, C to E; Supplemental Fig. S10).

We also explored the expression of ABA-responsive genes in WT and corresponding transgenic seeds. Compared with WT, the expression levels of *EM1* and *EM6* decreased in *Pro35S:MYC-MYB30* and *Pro35S:MYC-MYB30*^{C49W} but increased in *Pro35S:PYL4-GFP* plants. In *Pro35S:PYL4-GFP Pro35S:MYC-MYB30*, *EM1* and *EM6* expression was similar to that in *Pro35S:PYL4-GFP*. However, their expression in *Pro35S:PYL4-GFP Pro35S:MYC-MYB30*^{C49W} was more similar

to that in *Pro35S:MYC-MYB30*^{C49W} (Fig. 6F). Taken together, our results demonstrate that *S*-nitrosylation of MYB30 plays a critical role in repressing ABA signaling during germination.

Discussion

Seed dormancy and germination are important features that are crucial for agricultural production. NO has been shown to be an important molecule for breaking seed dormancy, and its function is closely related to the phytohormone ABA (Signorelli and Considine 2018). However, the antagonistic effect of NO on ABA can be divided into 2 aspects. On the one hand, NO negatively regulates the positive components of the ABA core signaling pathway. In brief, tyrosine nitration of PYLs attenuates their interaction with ABA, *S*-nitrosylation of SNF1-RELATED PROTEIN KINASE2 (SnRK2) kinases represses their kinase activity, and *S*-nitrosylation of ABI5 promotes its degradation. In addition, NO targets the Group VII ethylene response factors (ERFs) to the proteasome, which positively regulates the *ABI5* expression (Gibbs et al. 2014; Albertos et al. 2015; Castillo et al. 2015; Wang et al. 2015a, 2015b).

At the same time, the restriction of ABA by NO also indicates the modulation of ABA content during seed germination. The ABA content decreases during the germination, and the NO donor SNP can significantly promote the decrease of ABA content during seed germination, while the NO synthesis inhibitor PTIO inhibits this process (Liu et al. 2009). Our results demonstrate that MYB30 directly promotes the expression of ABA catabolism gene *CYP707A2* in response to NO, thus resulting in a decrease in ABA content and the release of dormancy. The mutation of the MYB30-binding site in the *CYP707A2* promoter dramatically repressed the increase in *CYP707A2* expression during germination and in response to NO (Fig. 2, I and J), and the increase of *CYP707A2* expression significantly reduced the dormancy phenotype of the *myb30* mutant (Fig. 2, F and G), suggesting a crucial role of the MYB30-CYP707A2 module in the regulation of seed dormancy.

In this study, we identified that the Cys-49 *S*-nitrosylation of MYB30 increases its transcriptional activity. First, *S*-nitrosylation enhances the enrichment of MYB30 to downstream target genes, such as *CYP707A2* and *EM1*. In addition, *S*-nitrosylation also promotes the interaction between MYB30 and ABI5, thus enhancing the repression of ABI5 transcriptional activity by MYB30 (Supplemental Fig. S9). This result indicates that *S*-nitrosylation also regulates the transcriptional activity of MYB30 by affecting its ability to interact with other proteins. Therefore, we cannot deny that there may also be regulation of the transcription function of MYB30 due to recruitment. According to our present results, we hypothesize that *S*-nitrosylation can regulate the transcription function of MYB30 in multiple ways. As the protein level of MYB30 during seed germination in response to ABA is also strictly controlled by multiple factors, such as ubiquitin E3 ligases RHA2b, MIEL1, and WD40 protein MYB30-INTERACTING WD40 PROTEIN1 (MIW1) (Zheng et al. 2018; Nie et al. 2022; Zhan et al. 2023), the effect of NO on MYB30 stability was also investigated. However, the application of the NO donor GSNO did not affect the protein level of MYB30 (Supplemental Fig. S5), suggesting that *S*-nitrosylation mainly regulates the transcriptional activity of MYB30.

Under our experimental conditions, *S*-nitrosylation at Cys-6, Cys-7, and Cys-49 residues of MYB30 was detected (Supplemental Fig. S6). As seen from the protein sequence of MYB30 (48-RCSKSCRLR-55), there are multiple lysine (K) and arginine (R) residues around Cys-49 and Cys-53, which will be cut during trypsin digestion, leading to the peptide containing Cys-49 and Cys-53 being difficult to be detected because of its too short sequence, especially for the Cys-53. Therefore, although Cys-53 is also predicted to be able to be *S*-nitrosylated (Kolbert and Lindermayr 2021), we failed to detect *S*-nitrosylation at Cys-53. Moreover, in our experimental system, the mutation of Cys-49 greatly reduced the *S*-nitrosylation of MYB30, indicating an important role of Cys-49 for MYB30 *S*-nitrosylation. However, the *S*-nitrosylation form of MYB30 protein can still be detected in seeds after Cys-49 mutation, indicating that Cys-49 is not the only *S*-nitrosylation site in the plants, which is consistent with the fact that we also detected *S*-nitrosylation at other residues. These data indicate that *S*-nitrosylation exists in multiple residues of MYB30 protein.

As a negative regulator of ABA signaling, the function of MYB30 is also limited by ABA signaling. Here, we found that the transcriptional activity of MYB30 is inhibited by PYL ABA receptors. Multiple PYLs interact with MYB30, and ABA restricts the transcriptional activity of MYB30 by promoting the PYL4-MYB30 interaction. *pyr1 pyl124* quintuple mutant exhibits less dormancy and higher *CYP707A2* expression in response to NO. However, the mutation of *MYB30* dramatically represses the dormancy phenotype and *CYP707A2* expression of the *pyr1 pyl124* mutant, suggesting that *MYB30* functions downstream of *PYLs* during seed dormancy and germination in response to NO. In contrast to ABA, NO-induced *S*-nitrosylation attenuates the PYL4-mediated repression of MYB30 by interfering with the PYL4-MYB30 interaction. The repression of PYL4 on MYB30^{C49W} is lower than that on MYB30, as the interaction between PYL4 and MYB30^{C49W} is weaker than the interaction between PYL4 and MYB30. Taken together, our work characterizes MYB30 as the executor of NO-induced seed germination. ABA and NO signals accurately control the dormancy and germination of seeds through antagonistic regulation of MYB30. NO-induced *S*-nitrosylation of MYB30 confers the accurate regulation of ABA content and signaling, thus precisely regulating seed dormancy and germination (Fig. 7).

However, MYB30 is not the only factor to be considered that is regulated by NO in the interaction between MYB30 and PYL4. As shown in Fig. 5, D to F, *S*-nitrosylation of

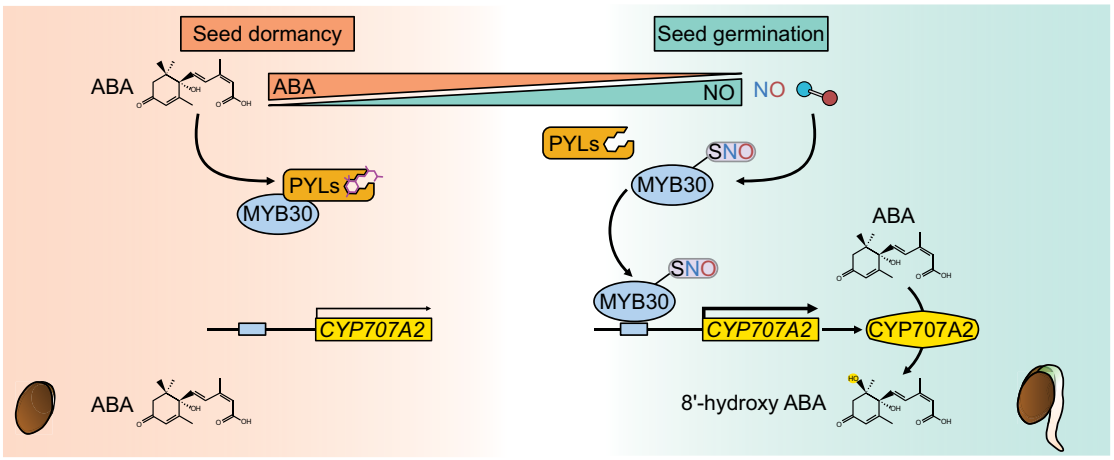

Figure 7. A proposed schematic model for MYB30 in regulating NO-promoted seed germination. During seed dormancy, ABA promotes the interaction between PYLs and MYB30 to repress the transcriptional activity of MYB30, thus preventing the expression of *CYP707A2*. After germination, the increased NO content causes the *S*-nitrosylation of MYB30. *S*-nitrosylation enhances the transcriptional activity of MYB30 by interfering with PYLs-MYB30 interaction, thus promoting the expression of *CYP707A2*, which leads to the decrease of ABA content and seed germination.

MYB30 reduces the interaction between MYB30 and PYL4, suggesting an important role of MYB30 *S*-nitrosylation in regulating MYB30-PYL4 interaction. But at the same time, *S*-nitrosylation reduces but not eliminates the interaction of MYB30 and PYL4, indicating that there may exist other ways of regulation. Based on the results of Castillo et al. (2015), both nitration and *S*-nitrosylation are also present in PYL4. Considering that *PYL4* expression is significantly increased during seed germination (Zhao et al. 2020) and that the content of NO is also increased (Liu et al. 2009), we hypothesize that the modification of PYL4 by NO may also exist during seed germination. As nitration represses the function of PYL4 as an ABA receptor by inhibiting the phosphatase activity of PP2Cs (Castillo et al. 2015) and ABA promotes the PYL4-MYB30 interaction to repress the function of MYB30, the nitration of PYL4 may also attenuate the function of PYL4 by interfering with the PYL4-MYB30 interaction. Meanwhile, although *S*-nitrosylation does not affect the inhibition of PYL4 on the phosphatase activity of HYPERSENSITIVE TO ABA1 (HAB1) (Castillo et al. 2015), *S*-nitrosylation of PYL4 may also function through other mechanisms to affect ABA signaling.

In addition to MYB30, another R2R3-MYB protein, MYB96, was also found to participate in the regulation of dormancy. Both MYB30 and MYB96 belong to the S1 R2R3-MYB subfamily (Dubos et al. 2010). It has been reported that MYB96 interacts with MYB30 and they both participate in the regulation of cuticular wax biosynthesis (Lee et al. 2017). However, in contrast to MYB30, MYB96 promotes seed dormancy through enhancing ABA biosynthesis by directly activating the expression of *NCED2* and *NCED6* (Lee et al. 2015a). Moreover, MYB96 directly regulates the transcription of *ABI4*, which also participates in seed dormancy regulation by regulating the balance of GA and ABA (Lee et al. 2015b; Shu et al. 2016). Although Lee et al. 2015b showed that MYB96 is not involved in the regulation of *CYP707A2* expression, they used 10-d-old seedlings but not dormant seeds. Considering that ABI4 directly represses the expression of *CYP707A2* by binding to its promoter (Shu et al. 2013) and MYB96 promotes *ABI4* expression, we hypothesize that MYB96 may repress the expression of *CYP707A2* through ABI4. Meanwhile, compared with the negative role of MYB30, MYB96 serves as a positive regulator of ABA signaling during seed germination. Considering that MYB96 suppresses the negative regulators of ABA through recruiting the histone modifier HISTONE DEACETYLASE15 (HDA15) to remove acetyl groups of histone H3 and H4 (Lee and Seo 2019), we hypothesized that MYB30 may play more roles in regulating gene expression.

Moreover, in addition to MYB30 and ABI4, *CYP707A2* may also be under the regulation of other types of transcription factors, as we also identified an E-box motif in the promoter of *CYP707A2*, which can be bound by bHLH transcription factors (Supplemental Fig. S4; Fisher and Goding 1992). At the same time, although the expression of *CYP707A2* induced by NO was inhibited in the *myb30* mutant, its expression still increased in response to NO, indicating that other components are involved in the regulation of *CYP707A2* by NO. Many reports have found that MYB and bHLH transcription factors can interact and jointly regulate downstream signals. For example, MYB30 can interact with PHY-INTERACTING FACTOR (PIF) transcription factors to regulate photomorphogenic development (Yan et al. 2020), and WD40 protein, MYB, and bHLH transcription factors form MYB–bHLH–WD40 (MBW) complexes to coregulate anthocyanin biosynthesis (Lloyd et al. 2017). We hypothesized that MYB30 may participate together with bHLH transcription factors in the regulation of *CYP707A2* expression by NO, thereby regulating the NO-mediated promotion of seed dormancy and germination.

Materials and methods

Plant materials and growth conditions

Arabidopsis (*Arabidopsis thaliana*) accession Columbia-0 was used as the WT. The *myb30-1* (*SALK_122884*), *myb30-2* mutants, and *MYB30*-overexpressing plants *Pro35S:MYC-MYB30* (*MYC-MYB30 #1* and *#2*) were described previously (Zheng et al. 2012; Liao et al. 2017). The *pyr1 pyl124* quintuple mutant was described previously (Park et al. 2009). The *gsnor1-3* mutant was described previously (Zhan et al. 2018).

To grow Arabidopsis seedlings, seeds were surface sterilized using 10% (*w*/*v*) sodium hypochlorite (NaClO) for 5 min and then sown on 1/2 MS medium (pH 5.8, 1% [*w*/*v*] sucrose and 0.3% [*w*/*v*] phytagel [Cat#P8169, Sigma-Aldrich]). After 3-d stratification at 4 °C, the seeds were transferred to a chamber with continuous white light at 100 μmol/m^2/s at 23 °C for 10 d. Arabidopsis plants were planted in a growth chamber under a 16-h light/8-h dark photoperiod at 100 μmol/m^2/s at 23 °C.

To grow *N. benthamiana*, the seeds were first sown on soil (nutrient soil/vermiculite; [1:1; *v*/*v*]) for 10 d and then the young seedlings were transplanted into culture boxes individually under a 16-h light/8-h dark photoperiod at 100 μmol/m^2/s at 23 °C.

Plasmid construction and generation of transgenic plants

To generate transgenic overexpression plants, the full-length coding sequences of *MYB30*, *CYP707A2*, and *PYL4* were cloned into the *pCambia1307-MYC* or *pCambia1300-GFP* vectors under the control of the cauliflower mosaic virus *35S* promoter to generate *Pro35S:MYC-MYB30*, *Pro35S:CYP707A2-GFP*, and *Pro35S:PYL4-GFP* using the ClonExpress Ultra One Step Cloning Kit (Cat#C115-01, Vazyme) (Nie et al. 2022; Lu et al. 2023). *MYB30*^{C49S} and *MYB30*^{C49W} were amplified form *Pro35S:MYC-MYB30* plasmid using the Mut Express II Fast Mutagenesis Kit V2 (Vazyme), and the primers were shown in Supplemental Table S1. The resulting constructs were introduced into Arabidopsis using *Agrobacterium tumefaciens*–mediated floral transformation and verified by immunoblotting. *Pro35S:PYL4-GFP Pro35S:MYC-MYB30* and *Pro35S:PYL4-GFP Pro35S:MYC-MYB30*^{C49W} were obtained by crossing *Pro35S:PYL4-GFP* with *Pro35S:MYC-MYB30* or *Pro35S:MYC-MYB30*^{C49W}. For complementation assays, 2,234 bp upstream of the *MYB30* translation start codon and full-length genome sequences of *MYB30* or *MYB30*^{C49W} were cloned into *pCambia1300* vector. The resulting construct was introduced into the *myb30-2* mutant. T_2 or subsequent generations of transgenic plants that are homozygous for a single insertion were used for all studies. At least 2 independent transgenic lines were analyzed. Unless specified otherwise, no apparent phenotype was observed in these transgenic plants under normal growth conditions.

Seed germination assays

For seed dormancy experiments, freshly harvested seeds were used for analysis. Sterilized seeds were plated on 0.3% (*w*/*v*) agar without or with 100 μM GSNO (Cat#487920, Sigma-Aldrich)/cPTIO (Cat#C221, Sigma-Aldrich). The plates were immediately transferred to a growth chamber without stratification in constant light at 100 μmol/m^2/s at 23 °C. Seeds were identified as germinated when a radicle had emerged from the seed coat (Shu et al. 2013). For seed germination assay, harvested seeds dried at room temperature for 4 wks were used for analysis. Seeds were plated on MS or MS containing 0.5 μM ABA (Cat#90769, Sigma-Aldrich). After stratification in the dark at 4 °C for 3 d, plates were transferred to the growth chamber.

RT-qPCR analysis

Total RNA was extracted from freshly harvested seeds and seeds that were imbibed in water or water containing 100 μM GSNO/cPTIO for indicated time by using an RNA extraction kit for polyphenolic-rich plant tissue (Cat#DP441, TIANGEN). The relative gene expression levels determined by RT-qPCR were normalized to the levels of *ACTIN2*. The primers used for RT-qPCR are listed in Supplemental Table S1.

Quantification of ABA

For analysis of ABA content in imbibed seeds, 150 mg of seeds were ground in liquid nitrogen and then homogenized in 2 mL methanol. Forty-five pM of $^2H_2$-ABA was added as an internal standard. After extraction at 20 °C overnight, the sample was centrifuged 10 min at 13,000 × *g* and the supernatant was dried under nitrogen gas and dissolved in 1 mL 5% (*v*/*v*) ammonia solution. The samples were purified by Oasis MAX strong anion-exchange column (Waters) and eluted by 4 mL methanol containing 5% (*v*/*v*) formic acid. The elution was dried under nitrogen gas and dissolved in 200 μL 80% (*v*/*v*) methanol. The sample was then subjected for ultraperformance liquid chromatography tandem mass spectrometry (LC-MS/MS) analysis (Jiang et al. 2016).

EMSA

GST-MYB30N (residues 1 to 149) fusion proteins were expressed in *E. coli* and then purified for use in EMSA. In brief, 0.5 mg of GST-MYB30N fusion proteins was incubated with biotin-labeled probe in 20 μL reaction mixtures (10 mM Tris-HCl, 50 mM KCl, 1 mM DTT, 50 ng/mL poly dI-dC, 2.5% [*v*/*v*] glycerol) at room temperature for 30 min. For competition, unlabeled unmutated and mutated probes used as competitors were added to the binding reactions, respectively. The reactions were separated on a 6% native polyacrylamide gel in 0.5 × TBE buffer (45 mM Tris, 45 mM boric acid, 1 mM EDTA, pH 8.3).

Transient expression assays in Arabidopsis protoplasts

The promoter sequence of *CYP707A2* and *EM1* were cloned into *pGreenII0800-LUC* vector which contains *REN* (*Renilla LUC*) gene driven by *35S* promoter as the internal control. The reporter was transiently expressed alone or with effectors in Arabidopsis protoplasts as described (Zheng et al

2018). For GSNO and cPTIO treatment, 100 μM GSNO or PTIO was added 3 h before the detection. Firefly LUC and REN activities were measured using the Dual-Luciferase Reporter Assay System (Promega) following the manufacturer's instructions. Relative LUC activity was calculated by normalizing against the REN activity. Primer sequences are listed in Supplemental Table S1.

ChIP-qPCR analysis

WT and the corresponding transgenic seeds imbibed in water or water containing 100 μM GSNO/cPTIO for 12 h were used for analysis of *CYP707A2*. For *EM1*, seeds grown on MS medium containing 0.5 μM ABA for 24 h were used for analysis. In brief, chromatin was immunoprecipitated by anti-MYC nanobody agarose beads (Cat#KTSM1336, AlpalifeBio). DNA fragments in both input and immunoprecipitated samples were quantified by qPCR. The *ACTIN2* promoter was used as a reference gene (Nie et al. 2022). At least 3 independent experiments were performed. The primers used for ChIP-qPCR are listed in Supplemental Table S1.

GUS staining and GUS activity

ProCYP707A2:GUS and *ProCYP707A2-m:GUS* transgenic plant seeds were imbibed in water or water containing 100 μM GSNO/cPTIO for 6 h and then stained in GUS staining solution (100 mM sodium phosphate buffer, pH 7.5, 10 mM EDTA, 0.5 mM potassium ferricyanide, 1 mM 5-bromochloro-3-indolyl-b-D-glucuronide, and 0.1% [*v*/*v*] Triton X-100). The samples were rinsed with 70% (*v*/*v*) ethanol several times to remove the chlorophyll, and images were then taken under a microscope (Leica DMI8, Leica Microsystems, Germany). The GUS activities of the transgenic seeds were assayed according to a method described previously (Lu et al. 2023).

In vitro S-nitrosylation assay

The in vitro *S*-nitrosylation assay was performed as described (Feng et al. 2013). In brief, 30 μg of His-tagged MYB30 or MYB30^{C49S} N-terminal recombinant proteins were incubated with 200 μM GSNO in the dark for 1 h. Protein was precipitated by acetone and resuspended in 300 μL blocking buffer I (250 mM HEPES, pH 7.7, 4 mM EDTA, 0.1 mM neocuproine, 2.5% [*v*/*v*] SDS, and 0.1% [*v*/*v*] S-methylmethane thiosulfonate). After incubation at 50 °C for 30 min, protein was precipitated and dissolved in 80 μL HENS buffer (250 mM HEPES, pH 7.7, 4 mM EDTA, 0.1 mM neocuproine, 1% [*v*/*v*] SDS) with the addition of 10 μL 500 mM sodium ascorbate (Asc) and 10 μL of 4 mM biotin-HPDP. After reaction at room temperature for 1 h, samples were separated by SDS–PAGE without boiling and analyzed by immunoblotting using anti-His (Cat#E12-004-3, EnoGene, 1:2,000) for input and anti-biotin antibody (Cat#7075, Cell Signaling Technology, 1:2,000) for *S*-nitrosylated MYB30.

In vivo S-nitrosylation assay

The in vivo *S*-nitrosylation assay was performed as described (Chen et al. 2020b). In brief, 0.25 g germination seeds were ground in liquid nitrogen and dissolved in 1 mL HEN buffer (250 mM HEPES, pH 7.7, 1 mM EDTA, 0.1 mM neocuproine, protease inhibitor cocktail). Then 200 μg protein was incubated with blocking buffer I at 50 °C for 1 h. Protein was precipitated with cold acetone and resuspended in 170 μL of HENS buffer. Protein was labeled at room temperature for 1 h by addition of 10 μL of 1 M Asc and 20 μL of 4 mM biotin-HPDP. After precipitation and wash with acetone, sample was resuspended in 400 μL HENS buffer and neutralized with 800 μL of neutralization buffer (25 mM HEPES, pH 7.7, 100 mM NaCl, 1 mM EDTA, and 0.5% [*v*/*v*] Triton X-100). The sample was incubated with 30 μL of streptavidin beads (Cat #29202, Thermo Scientific) at 4 °C overnight. The beads were washed 4 times with washing buffer (25 mM HEPES, pH 7.7, 600 mM NaCl, 1 mM EDTA, and 0.5% [*v*/*v*] Triton X-100). The proteins were then analyzed by immunoblotting using an anti-biotin antibody.

BiFC and LCI assays

The full-length coding sequences of *PYL* genes were cloned into the *pSPYNE* vector (containing the N-terminal of YFP), and *MYB30* without stop codon was cloned into the *pSPYCE* vector (containing the C-terminal of YFP) using the ClonExpress Ultra One Step Cloning Kit to produce YNE-PYLs and MYB30-YCE (Walter et al. 2004; Lu et al. 2023). The resulting constructs were coexpressed in *N. benthamiana* leaves for 2 d. YFP fluorescence signals were detected using a laser scanning confocal microscope (ZEISS LSM980; lasers: 488 nm, 15%; 560 nm, 15%; gains: 600; pinhole: 100 μm).

For the LCI assay, nLUC-PYL4 and cLUC-MYB30 were co-transformed into *N. benthamiana* for 2 d. A total of 100 μM D-luciferin was sprayed on the leaves before image collection by a CCD camera. For the ABA treatment, 10 μM ABA was injected into the 2-d transfection leaves for 3 h.

Co-IP assays

For PYL4-MYB30 interaction identification, *Pro35S:PYL4-GFP* and *Pro35S:MYC-MYB30* constructs was transiently expressed in *N. benthamiana* leaves. For the ABA treatment, 10 μM ABA was injected into the 2-d transfection leaves for 3 h. For the interaction identified in seeds, *Pro35S:PYL4-GFP*, *Pro35S:MYC-MYB30*, *Pro35S:PYL4-GFP Pro35S:MYC-MYB30*, and *Pro35S:PYL4-GFP Pro35S:MYC-MYB30*^{C49W} seeds imbibed in water for 24 h were used for protein extract. Proteins were extracted using IP buffer (150 mM NaCl, 25 mM Tris-HCl, pH 7.5, 0.2% [*v*/*v*] Nonidet P-40, 1 mM phenylmethylsulfonyl fluoride (PMSF), and 1× protease inhibitor cocktail) and purified with anti-GFP agarose (Cat#KTSM1334, AlpalifeBio). The resulting extractions were then detected using anti-GFP (Cat#D110008, Sangon Biotech, 1:2,000) and anti-MYC (Cat#CW0229, CWBIO, 1:2,000) antibodies, respectively.

In vitro pull-down assays

The coding sequence of *PYL4* was cloned into the *pET28a* vector for His-tag-fused protein purification, whereas

MYB30N (residues 1 to 149) was cloned into the *pGEX-6P-1* vector for a GST tag. For in vitro pull-down assays, indicated proteins were included in the pull-down buffer (50 mM Tris-HCl, pH 7.5, 100 mM NaCl, 0.2% [*v*/*v*] glycerol, 0.6% [*v*/*v*] Triton X-100, 0.1 mM EDTA) for incubation; then, GST and GST-MYB30N proteins were isolated using GST antibody-conjugated agarose. After washing 3 times using wash buffer (50 mM Tris-HCl, pH 7.5, 300 mM NaCl, 1% [*v*/*v*] Triton X-100, 0.1 mM EDTA), GST, GST-MYB30N, and GST-MYB30N-interacting proteins were detected through immunoblot analysis using anti-GST (Cat#AE006, ABclonal, 1:2,000) and anti-His antibodies, respectively. For GSNO treatment, final concentration of 200 μM GSNO was added to the extraction buffer for 3 h in the dark before the MYB30 protein was purified by GST agarose (Chen et al. 2022).

Mass spectrometry analysis

Mass spectrometric identification of *S*-nitrosylated Cys residues was carried out according to a previous report (Chen et al. 2020b). In brief, 30 μg GST-MYB30N (residues 1 to 149) recombinant proteins were labeled with biotinemaleimide (Cat#B1267, Sigma-Aldrich). The biotinylated protein was digested with Trypsin (Cat#V5280, Promega) and then analyzed by LC-MS/MS using a Thermo Fisher Finnigan linear ion trap quadrupole mass spectrometer in line with a Thermo Fisher Finnigan Surveyor MS Pump Plus HPLC system. The raw data were searched against the GST-MYB30N protein sequence using pFIND software (Chen et al. 2020b). Cys biotinylation (451.200 Da) was included in the search as the variable modification.

Statistical analysis

Data are means ± SD of 3 biological replicates, and the asterisks indicate statistically significant differences (*$P < 0.05$, **$P < 0.01$, Student's *t* test). Bars with different letters indicate significant differences at $P < 0.05$ by ANOVA with Tukey's multiple comparison test or ordinary 1-way test. Detailed statistical analysis results are in Supplemental Data Set S1.

Accession numbers

Sequence data can be found in the Arabidopsis Genome Initiative or GenBank/EMBL databases under accession numbers: *MYB30* (At3g28910), *ABA1* (At5g67030), *AAO3* (At2g27150), *NCED3* (At3g14440), *NCED9* (At1g78390), *CYP707A1* (At4g19230), *CYP707A2* (At2g29090), *CYP707A3* (At5g45340), *GSNOR* (At5g43940), *PYL3* (At1g73000), *PYL4* (At2g38310), *PYL8* (At5g53160), *PYL10* (At4g27920), *PYL11* (At5g45860), *PYL12* (At5g45870), *MYB3* (AT1G22640), *EM1* (At3g51810), and *EM6* (At2g40170).

Acknowledgments

We thank the anonymous reviewers for their thoughtful reviews and constructive suggestions which have improved this paper.

Author contributions

Hu.Z. and Y.Z. designed the research; Ho.Z., L.M., and J.S. performed the research; Hu.Z. and Ho.Z. analyzed the data; and Y.Z. wrote the manuscript.

Supplemental data

The following materials are available in the online version of this article.

Supplemental Figure S1. Expression of *MYB30* in *myb30* mutants and *MYB30*-overexpressing plants.

Supplemental Figure S2. The dormancy phenotype of *MYB30*-overexpressing seeds.

Supplemental Figure S3. Expression of ABA metabolism genes in WT and *myb30-2* seeds.

Supplemental Figure S4. Analysis of *CYP707A2* promoter and the expression of *MYB30* and *CYP707A2*.

Supplemental Figure S5. MYB30 expression and stability under GSNO treatment.

Supplemental Figure S6. Mapping of MYB30N *S*-nitrosylation sites in MYB30N protein.

Supplemental Figure S7. *MYB30* transcript and protein levels in WT and multiple *MYB30* transgenic plants.

Supplemental Figure S8. Control of BiFC and LCI assays and Co-IP analysis of PYL4-MYB30 interaction in *N. benthamiana*.

Supplemental Figure S9. *S*-nitrosylation facilitates MYB30 to repress the transcriptional activity of ABI5.

Supplemental Figure S10. The ABA phenotype of second lines of MYB30- and PYL4-related transgenic plants.

Supplemental Table S1. Primer sequences used in the manuscript.

Supplemental Data Set S1. Statistical analysis results.

Funding

This work was supported by the Natural Science Foundation of Henan (212300410022) and the National Natural Science Foundation of China (31872656 and 32170295).

Conflict of interest statement. None declared.

References

Albertos P, Romero-Puertas MC, Tatematsu K, Mateos I, Sanchez-Vicente I, Nambara E, Lorenzo O. S-nitrosylation triggers ABI5 degradation to promote seed germination and seedling growth. Nat Comm. 2015:**6**(1):8669. https://doi.org/10.1038/ncomms9669

Arc E, Galland M, Godin B, Cueff G, Rajjou L. Nitric oxide implication in the control of seed dormancy and germination. Front Plant Sci. 2013:**4**:346. https://doi.org/10.3389/fpls.2013.00346

Astier J, Rasul S, Koen E, Manzoor H, Besson-Bard A, Lamotte O, Jeandroz S, Durner J, Lindermayr C, Wendehenne D. S-nitrosylation: an emerging post-translational protein modification in plants. Plant Sci. 2011:**181**(5):527–533. https://doi.org/10.1016/j.plantsci.2011.02.011

Bentsink L, Koornneef M. Seed dormancy and germination. Arabidopsis Book. 2008:**6**:e0119. https://doi.org/10.1199/tab.0119

Bethke PC, Gubler F, Jacobsen JV, Jones RL. Dormancy of Arabidopsis seeds and barley can be broken by nitric oxide. Planta 2004:**219**(5): 847–855. https://doi.org/10.1007/s00425-004-1282-x

Bethke PC, Libourel IG, Jones RL. Nitric oxide reduces seed dormancy in Arabidopsis. J Exp Bot. 2006:**57**(3):517–526. https://doi.org/10.1093/jxb/erj060

Castillo M-C, Lozano-Juste J, Gonzalez-Guzman M, Rodriguez L, Rodriguez PL, Leon J. Inactivation of PYR/PYL/RCAR ABA receptors by tyrosine nitration may enable rapid inhibition of ABA signaling by nitric oxide in plants. Sci Signal. 2015:**8**(392):ra89. https://doi.org/10.1126/scisignal.aaa7981

Chen K, Li GJ, Bressan RA, Song CP, Zhu JK, Zhao Y. Abscisic acid dynamics, signaling and functions in plants. J Integr Plant Biol. 2020a:**62**(1):25–54. https://doi.org/10.1111/jipb.12899

Chen L, Su NS, Song CP, Zhou JM, Li J, Zuo J. Nitric oxide negatively regulates gibberellin signaling to coordinate growth and salt tolerance in Arabidopsis. J Genet Genomics. 2022:**49**(8):756–765. https://doi.org/10.1016/j.jgg.2022.02.023

Chen L, Wu R, Feng J, Feng T, Wang C, Hu J, Zhan N, Li Y, Ma X, Ren B, et al. Transnitrosylation mediated by the non-canonical catalase ROG1 regulates nitric oxide signaling in plants. Dev Cell. 2020b:**53**(4):444e457. https://doi.org/10.1016/j.devcel.2020.03.020

Dubos C, Stracke R, Grotewold E, Weisshaar B, Martin C, Lepiniec L. MYB transcription factors in Arabidopsis. Trends Plant Sci. 2010:**15**(10):573–581. https://doi.org/10.1016/j.tplants.2010.06.005

Feng J, Chen L, Zuo J. Protein S-nitrosylation in plants: current progresses and challenges. J Integr Plant Biol. 2019:**61**(12):1206–1223. https://doi.org/10.1111/jipb.12780

Feng J, Wang C, Chen Q, Chen H, Ren B, Li X, Zuo J. S-nitrosylation of phosphotransfer proteins represses cytokinin signaling. Nat Commun. 2013:**4**(1):1529. https://doi.org/10.1038/ncomms2541

Fisher F, Goding CR. Single amino acid substitutions alter helix-loop-helix protein specificity for bases flanking the core CANNTG motif. EMBO J. 1992:**11**(11):4103–4109. https://doi.org/10.1002/j.1460-2075.1992.tb05503.x

Gibbs DJ, MdIsa N, Movahedi M, Lozano-Juste J, Mendiondo GM, Berckhan S, et al. Nitric oxide sensing in plants is mediated by proteolytic control of group VII ERF transcription factors. Mol Cell. 2014:**53**(3):369–379. https://doi.org/10.1016/j.molcel.2013.12.020

Graeber K, Nakabayashi K, Miatton E, Leubner-Metzger G, Soppe WJ. Molecular mechanisms of seed dormancy. Plant Cell Environ. 2012:**35**(10):1769–1786. https://doi.org/10.1111/j.1365-3040.2012.02542.x

Jiang Z, Xu G, Jing Y, Tang W, Lin R. Phytochrome B and REVEILLE1/2-mediated signalling controls seed dormancy and germination in Arabidopsis. Nat Commun. 2016:**7**(1):12377. https://doi.org/10.1038/ncomms12377

Kolbert Z, Lindermayr C. Computational prediction of NO-dependent posttranslational modifications in plants: current status and perspectives. Plant Physiol Biochem. 2021:**167**:851–861. https://doi.org/10.1016/j.plaphy.2021.09.011

Lee HG, Kim J, Suh MC, Seo PJ. The MIEL1 E3 ubiquitin ligase negatively regulates cuticular wax biosynthesis in Arabidopsis stems. Plant Cell Physiol. 2017:**58**(11):1249–1259. https://doi.org/10.1093/pcp/pcx116

Lee HG, Lee K, Seo PJ. The Arabidopsis MYB96 transcription factor plays a role in seed dormancy. Plant Mol Biol. 2015b:**87**(4-5): 371–381. https://doi.org/10.1007/s11103-015-0283-4

Lee HG, Seo PJ. MYB96 recruits the HDA15 protein to suppress negative regulators of ABA signaling in Arabidopsis. Nat Commun. 2019:**10**(1):1713. https://doi.org/10.1038/s41467-019-09417-1

Lee JH, Yoon HJ, Terzaghi W, Martinez C, Dai M, Li J, Byun MO, Deng XW. DWA1 and DWA2, two Arabidopsis DWD protein components of CUL4-based E3 ligases, act together as negative regulators in ABA signal transduction. Plant Cell. 2010:**22**(6):1716–1732. https://doi.org/10.1105/tpc.109.073783

Lee K, Lee HG, Yoon S, Kim HU, Seo PJ. The Arabidopsis MYB96 transcription factor is a positive regulator of ABSCISIC ACID-INSENSITIVE4 in the control of seed germination. Plant Physiol. 2015a:**168**(2):677–689. https://doi.org/10.1104/pp.15.00162

Li L, Yu X, Thompson A, Guo M, Yoshida S, Asami T, Chory J, Yin Y. Arabidopsis MYB30 is a direct target of BES1 and cooperates with BES1 to regulate brassinosteroid-induced gene expression. Plant J. 2009:**58**(2):275–286. https://doi.org/10.1111/j.1365-313X.2008.03778.x

Liao C, Zheng Y, Guo Y. MYB30 transcription factor regulates oxidative and heat stress responses through ANNEXIN-mediated cytosolic calcium signaling in Arabidopsis. New Phytol. 2017:**216**(1):163–177. https://doi.org/10.1111/nph.14679

Liu H, Stone SL. Abscisic acid increases Arabidopsis ABI5 transcription factor levels by promoting KEG E3 ligase self-ubiquitination and proteasomal degradation. Plant Cell. 2010:**22**(8):2630–2641. https://doi.org/10.1105/tpc.110.076075

Liu Y, Shi L, Ye N, Liu R, Jia W, Zhang J. Nitric oxide-induced rapid decrease of abscisic acid concentration is required in breaking seed dormancy in Arabidopsis. New Phytol. 2009:**183**(4):1030–1042. https://doi.org/10.1111/j.1469-8137.2009.02899.x

Lloyd A, Brockman A, Aguirre L, Campbell A, Bean A, Cantero A, Gonzalez A. Advances in the MYB-bHLH-WD repeat (MBW) pigment regulatory model: addition of a WRKY factor and co-option of an anthocyanin MYB for betalain regulation. Plant Cell Physiol. 2017:**58**(9):1431–1441. https://doi.org/10.1093/pcp/pcx075

Lopez-Molina L, Mongrand S, McLachlin DT, Chait BT, Chua NH. ABI5 acts downstream of ABI3 to execute an ABA-dependent growth arrest during germination. Plant J. 2002:**32**(3):317–328. https://doi.org/10.1046/j.1365-313X.2002.01430.x

Lozano-Juste J, León J. Enhanced abscisic acid-mediated responses in nia1nia2noa1–2 triple mutant impaired in NIA/NR- and AtNOA1-dependent nitric oxide biosynthesis in Arabidopsis. Plant Physiol. 2010:**152**(2):891–903. https://doi.org/10.1104/pp.109.148023

Lu KK, Song RF, Guo JX, Zhan GY, Zuo JX, Chen HH, Liao CY, Hu XY, Ren F, Lu YT, et al. Cycc1; 1-WRKY75 complex-mediated transcriptional regulation of SOS1 controls salt stress tolerance in Arabidopsis. Plant Cell. 2023:**35**(7):2570–2591. https://doi.org/10.1093/plcell/koad105

Ma Y, Szostkiewicz I, Korte A, Moes D, Yang Y, Christmann A, Grill E. Regulators of PP2C phosphatase activity function as abscisic acid sensors. Science 2009:**324**(5930):1064–1068. https://doi.org/10.1126/science.1172408

Matakiadis T, Alboresi A, Jikumaru Y, Tatematsu K, Pichon O, Renou JP, Kamiya Y, Nambara E, Truong HN. The Arabidopsis abscisic acid catabolic gene CYP707A2 plays a key role in nitrate control of seed dormancy. Plant Physiol. 2009:**149**(2):949–960. https://doi.org/10.1104/pp.108.126938

Nie K, Zhao H, Wang X, Niu Y, Zhou H, Zheng Y. The MIEL1-ABI5/MYB30 regulatory module fine tunes abscisic acid signaling during seed germination. J Integr Plant Biol. 2022:**64**(4):930–941. https://doi.org/10.1111/jipb.13234

Okamoto M, Kuwahara A, Seo M, Kushiro T, Asami T, Hirai N, Kamiya Y, Koshiba T, Nambara E. CYP707A1 and CYP707A2, which encode abscisic acid 8′-hydroxylases, are indispensable for proper control of seed dormancy and germination in Arabidopsis. Plant Physiol. 2006:**141**(1):97–107. https://doi.org/10.1104/pp.106.079475

Palmer ZJ, Duncan RR, Johnson JR, Lian LY, Mello LV, Booth D, Barclay JW, Graham ME, Burgoyne RD, Prior IA, et al. S-nitrosylation of syntaxin 1 at Cys(145) is a regulatory switch controlling Munc18-1 binding. Biochem J. 2008:**413**(3):479–491. https://doi.org/10.1042/BJ20080069

Park SY, Fung P, Nishimura N, Jensen DR, Fujii H, Zhao Y, Lumba S, Santiago J, Rodrigues A, Chow TF, et al. Abscisic acid inhibits type 2C protein phosphatases via the PYR/PYL family of START proteins. Science 2009:**324**(5930):1068–1071. https://doi.org/10.1126/science.1173041

Piskurewicz U, Jikumaru Y, Kinoshita N, Nambara E, Kamiya Y, Lopez-Molina L. The gibberellic acid signaling repressor RGL2 inhibits Arabidopsis seed germination by stimulating abscisic acid synthesis and ABI5 activity. Plant Cell. 2008:**20**(10):2729–2745. https://doi.org/10.1105/tpc.108.061515

Raffaele S, Vailleau F, Léger A, Joubès J, Miersch O, Huard C, Blée E, Mongrand S, Domergue F, Roby D. A MYB transcription factor regulates very-long-chain fatty acid biosynthesis for activation of the hypersensitive cell death response in Arabidopsis. Plant Cell. 2008:**20**(3):752–767. https://doi.org/10.1105/tpc.107.054858

Sano N, Marion-Poll A. ABA metabolism and homeostasis in seed dormancy and germination. Int J Mol Sci. 2021:**22**(10):5069. https://doi.org/10.3390/ijms22105069

Seo KI, Lee JH, Nezames CD, Zhong S, Song E, Byun MO, Deng XW. ABD1 is an Arabidopsis DCAF substrate receptor for CUL4-DDB1-based E3 ligases that acts as a negative regulator of abscisic acid signaling. Plant Cell. 2014:**26**(2):695–711. https://doi.org/10.1105/tpc.113.119974

Seo M, Hanada A, Kuwahara A, Endo A, Okamoto M, Yamauchi Y, North H, Marion-Poll A, Sun TP, Koshiba T, et al. Regulation of hormone metabolism in Arabidopsis seeds: phytochrome regulation of abscisic acid metabolism and abscisic acid regulation of gibberellin metabolism. Plant J. 2006:**48**(3):354–366. https://doi.org/10.1111/j.1365-313X.2006.02881.x

Shu K, Liu XD, Xie Q, He ZH. Two faces of one seed: hormonal regulation of dormancy and germination. Mol Plant. 2016:**9**(1):34–45. https://doi.org/10.1016/j.molp.2015.08.010

Shu K, Zhang H, Wang S, Chen M, Wu Y, Tang S, Liu C, Feng Y, Cao X, Xie Q. ABI4 regulates primary seed dormancy by regulating the biogenesis of abscisic acid and gibberellins in Arabidopsis. PLoS Genet. 2013:**9**(6):e1003577. https://doi.org/10.1371/journal.pgen.1003577

Signorelli S, Considine MJ. Nitric oxide enables germination by a four-pronged attack on ABA-induced seed dormancy. Front Plant Sci. 2018:**9**:296. https://doi.org/10.3389/fpls.2018.00296

Söderman EM, Brocard IM, Lynch TJ, Finkelstein RR. Regulation and function of the arabidopsis ABA-insensitive4 gene in seed and abscisic acid response signaling networks. Plant Physiol. 2000:**124**(4):1752–1765. https://doi.org/10.1104/pp.124.4.1752

Vailleau F, Daniel X, Tronchet M, Montillet JL, Triantaphylidès C, Roby D. R2R3-MYB gene, AtMYB30, acts as a positive regulator of the hypersensitive cell death program in plants in response to pathogen attack. Proc Natl Acad Sci USA. 2002:**99**(15):10179–10184. https://doi.org/10.1073/pnas.152047199

Wang P, Du Y, Hou Y-J, Zhao Y, Hsu C-C, Yuan F, et al. Nitric oxide negatively regulates abscisic acid signaling in guard cells by S-nitrosylation of OST1. Proc Natl Acad Sci U.S.A. 2015a:**112**(2):613–618. https://doi.org/10.1073/pnas.1423481112

Wang P, Zhu JK, Lang Z. Nitric oxide suppresses the inhibitory effect of abscisic acid on seed germination by S-nitrosylation of SnRK2 proteins. Plant Signal Behav. 2015b:**10**(6):e1031939. https://doi.org/10.1080/15592324.2015.1031939

Wang Z, Ren Z, Cheng C, Wang T, Ji H, Zhao Y, Deng Z, Zhi L, Lu J, Wu X, et al. Counteraction of ABA-mediated inhibition of seed germination and seedling establishment by ABA signaling terminator in Arabidopsis. Mol Plant. 2020:**13**(9):1284–1297. https://doi.org/10.1016/j.molp.2020.06.011

Walter M, Chaban C, Schütze K, Batistic O, Weckermann K, Näke C, Blazevic D, Grefen C, Schumacher K, Oecking C, et al. Visualization of protein interactions in living plant cells using bimolecular fluorescence complementation. Plant J. 2004:**40**(3):428–438. https://doi.org/10.1111/j.1365-313X.2004.02219.x

Yan Y, Li C, Dong X, Li H, Zhang D, Zhou Y, Jiang B, Peng J, Qin X, Cheng J, et al. MYB30 is a key negative regulator of Arabidopsis photomorphogenic development that promotes PIF4 and PIF5 protein accumulation in the light. Plant Cell. 2020:**32**(7):2196–2215. https://doi.org/10.1105/tpc.19.00645

Zhan N, Wang C, Chen L, Yang H, Feng J, Gong X, Ren B, Wu R, Mu J, et al. S-nitrosylation targets GSNO reductase for selective autophagy during hypoxia responses in plants. Mol Cell. 2018:**71**(1):142–154.e6. https://doi.org/10.1016/j.molcel.2018.05.024

Zhan Q, Shen J, Nie K, Zheng Y. MIW1 participates in ABA signaling through the regulation of MYB30 in Arabidopsis. Plant Sci. 2023:**332**:111717. https://doi.org/10.1016/j.plantsci.2023.111717

Zhao H, Nie K, Zhou H, Yan X, Zhan Q, Zheng Y, Song CP. ABI5 modulates seed germination via feedback regulation of the expression of the PYR/PYL/RCAR ABA receptor genes. New Phytol. 2020:**228**(2):596–608. https://doi.org/10.1111/nph.16713

Zheng Y, Chen Z, Ma L, Liao C. The ubiquitin E3 ligase RHA2b promotes degradation of MYB30 in abscisic acid signaling. Plant Physiol. 2018:**178**(1):428–440. https://doi.org/10.1104/pp.18.00683

Zheng Y, Schumaker KS, Guo Y. Sumoylation of transcription factor MYB30 by the small ubiquitin-like modifier E3 ligase SIZ1 mediates abscisic acid response in *Arabidopsis thaliana*. Proc Natl Acad Sci USA. 2012:**109**(31): 12822–12827. https://doi.org/10.1073/pnas.1202630109